



MODIFICATION OF A MODULATION RECOGNITION ALGORITHM  
TO ENABLE MULTI-CARRIER RECOGNITION

THESIS

Angela M. Waters, Second Lieutenant, USAF

AFIT/GE/ENG/05-23

DEPARTMENT OF THE AIR FORCE  
AIR UNIVERSITY

**AIR FORCE INSTITUTE OF TECHNOLOGY**

Wright-Patterson Air Force Base, Ohio

APPROVED FOR PUBLIC RELEASE; DISTRIBUTION UNLIMITED.

The views expressed in this thesis are those of the author and do not reflect the official policy or position of the United States Air Force, Department of Defense, or the United States Government.

MODIFICATION OF A MODULATION RECOGNITION  
ALGORITHM TO ENABLE MULTI-CARRIER  
RECOGNITION

THESIS

Presented to the Faculty  
Department of Electrical and Computer Engineering  
Graduate School of Engineering and Management  
Air Force Institute of Technology  
Air University  
Air Education and Training Command  
In Partial Fulfillment of the Requirements for the  
Degree of Master of Science in Electrical Engineering

Angela M. Waters, B.S.E.E., B.S.C.P.  
Second Lieutenant, USAF

March 2005

APPROVED FOR PUBLIC RELEASE; DISTRIBUTION UNLIMITED.

MODIFICATION OF A MODULATION RECOGNITION  
ALGORITHM TO ENABLE MULTI-CARRIER  
RECOGNITION

Angela M. Waters, B.S.E.E., B.S.C.P.  
Second Lieutenant, USAF

Approved:

/signed/

11 Mar 2005

\_\_\_\_\_  
Dr. Michael A. Temple (Chairman)

\_\_\_\_\_  
date

/signed/

11 Mar 2005

\_\_\_\_\_  
Dr. Steven C. Gustafson (Member)

\_\_\_\_\_  
date

/signed/

11 Mar 2005

\_\_\_\_\_  
Dr. Robert F. Mills (Member)

\_\_\_\_\_  
date

*Abstract*

Modulation recognition is important for both military and commercial communication applications, particularly in cases where enhanced situation awareness and/or channel assessment is required to mitigate intentional or collateral interference. Modulation recognition via template matching or statistical analysis is a key aspect of non-cooperative (non-matched filtering) signal interception, classification, and exploitation.

This research concerns the evaluation and modification of a conventional Digitally Modulated Signal Recognition Algorithm (DMRA) to enable multi-carrier, Orthogonal Frequency Division Multiplexing (OFDM), waveform recognition. The original DMRA architecture was developed to classify binary and 4-ary communication signals for three fundamental data modulations, i.e., Amplitude Shift Keying (ASK), Phase Shift Keying (PSK), and Frequency Shift Keying (FSK). By adding an additional key feature and threshold to the original DMRA architecture, a modified DMRA architecture is developed to enable the reliable recognition of OFDM waveforms.

Simulation results for the modified DMRA architecture show a 95.25% success rate for OFDM waveform recognition at a signal-to-noise ratio (SNR) of 11.0 *dB*. When operated under scenarios where FSK signals are neither present nor considered an alternative, the modified DMRA architecture yields success rates of 100%, 98.25%, and 98.25% for classifying PSK2, PSK4, and OFDM, respectively, at a SNR of 5.0 *dB*.

## *Acknowledgements*

I am very grateful for the support of my family and friends that made this effort possible. A special thanks to Dr. Temple, for your guidance and encouragement.

Angela M. Waters

## *Table of Contents*

	Page
Abstract . . . . .	iv
Acknowledgements . . . . .	v
List of Figures . . . . .	ix
List of Tables . . . . .	xi
 I. Introduction . . . . .	 1
1.1 Introduction . . . . .	1
1.2 Problem Statement . . . . .	1
1.3 Research Assumptions . . . . .	2
1.4 Research Scope . . . . .	2
1.5 Research Approach . . . . .	2
1.6 Materials and Equipment . . . . .	3
1.7 Thesis Organization . . . . .	4
 II. Background . . . . .	 5
2.1 Introduction . . . . .	5
2.2 Signal Types: Fundamental Modulations . . . . .	5
2.2.1 Amplitude Shift Keying (ASK) . . . . .	5
2.2.2 Phase Shift Keying (PSK) . . . . .	6
2.2.3 Frequency Shift Keying (FSK) . . . . .	6
2.3 Orthogonal Frequency Division Multiplexing (OFDM) . . . . .	6
2.4 Modulation Recognition . . . . .	8
2.5 Digitally Modulated Signal Recognition Algorithm (DMRA) . . . . .	9
2.6 Key Feature Extraction . . . . .	10
2.6.1 Maximum Power Spectral Density Feature ( $\gamma_{max}$ ) . . . . .	10
2.6.2 Absolute Phase Feature ( $\sigma_{AP}$ ) . . . . .	10
2.6.3 Direct Phase ( $\sigma_{DP}$ ) . . . . .	11
2.6.4 Absolute Amplitude ( $\sigma_{AA}$ ) . . . . .	11
2.6.5 Absolute Frequency ( $\sigma_{AF}$ ) . . . . .	12
2.6.6 Classification . . . . .	12
2.6.7 Confusion Matrices . . . . .	12
2.7 Summary . . . . .	13

	Page
III. Methodology . . . . .	14
3.1 Introduction . . . . .	14
3.2 Modulated Signals: Fundamental Modulation Parameters . . . . .	14
3.3 Modulated Signals: OFDM . . . . .	16
3.4 Bandpass Filter Characteristics and SNR Calculation . . . . .	16
3.5 Signal Qualifying Parameters . . . . .	18
3.6 Key Feature Extraction . . . . .	18
3.7 DMRA Processing . . . . .	18
3.7.1 DMRA Development for Fundamental Modulations . . . . .	19
3.7.2 DMRA Operation for Fundamental Modulations . . . . .	19
3.8 Introduction of OFDM into DMRA . . . . .	20
3.9 Summary . . . . .	20
IV. Results and Analysis . . . . .	22
4.1 Introduction . . . . .	22
4.2 Fundamental Modulation Time Waveforms . . . . .	22
4.2.1 Normalized Centered Amplitude Response ( $a_{cn}$ ) . . . . .	22
4.2.2 Normalized Centered Nonlinear Phase Response ( $\phi_{NL}$ ) . . . . .	23
4.2.3 Normalized Centered Frequency Response ( $f_N$ ) . . . . .	23
4.3 Initial DMRA Development for Fundamental Modulations . . . . .	25
4.3.1 Dependence of $\gamma_{max}$ on SNR . . . . .	26
4.3.2 Dependence of $\sigma_{AP}$ on SNR, ( $\gamma_{max} \geq t_\gamma$ ) . . . . .	27
4.3.3 Dependence of $\sigma_{DP}$ on SNR, ( $\sigma_{AP} \leq t_{AP}$ ) . . . . .	29
4.3.4 Dependence of $\sigma_{AA}$ on SNR, ( $\sigma_{DP} \leq t_{DP}$ ) . . . . .	29
4.3.5 Dependence of $\sigma_{AF}$ on SNR, ( $\gamma_{max} < t_\gamma$ ) . . . . .	30
4.3.6 Summary of Initial DMRA Threshold Values . . . . .	30
4.4 Operational DMRA Performance: Fundamental Modulations . . . . .	33
4.4.1 Confusion Matrix Analysis . . . . .	33
4.5 Introduction of QAM-OFDM Waveform . . . . .	34
4.5.1 Unmodified DMRA Performance: OFDM Waveform Present . . . . .	34
4.5.2 Analysis of Unmodified DMRA with OFDM Waveform . . . . .	36
4.5.3 Modified DMRA Performance: OFDM Waveform Present . . . . .	38
4.5.4 OFDM Recognition Results . . . . .	38
4.6 Summary . . . . .	40

	Page
V. Conclusions . . . . .	43
5.1 Summary . . . . .	43
5.2 Recommendations for Future Research . . . . .	43
5.2.1 Improvement of Fundamental Modulation Performance . . . . .	43
5.2.2 Additional Waveform Recognition . . . . .	44
Appendix A. . . . .	45
A.1 4-ary Modulation Waveforms and Instantaneous Plots . . . . .	45
Bibliography . . . . .	49

## *List of Figures*

Figure		Page
1.	Fundamental Modulation DMRA Decision Tree [7] . . . . .	9
2.	Modulation Recognition Process . . . . .	15
3.	Filter Response of 8 <sup>th</sup> -Order Chebyshev Filter . . . . .	17
4.	Sample Feature Threshold Determination . . . . .	20
5.	Time Domain Waveforms for Binary Modulations . . . . .	23
6.	Normalized Centered Instantaneous Amplitude Response, $a_{cn}$ , for Binary Modulated Waveforms of Figure 5 . . . . .	24
7.	Normalized Centered Nonlinear Phase Response, $\phi_{NL}$ , for Binary Modulated Waveforms of Figure 5 . . . . .	24
8.	Nonlinear Phase Response, $\phi_{NL2}$ , for Binary Modulated Wave- forms of Figure 5 . . . . .	25
9.	Normalized Centered Frequency Response, $f_N$ , for Binary Mod- ulated Waveforms of Figure 5 . . . . .	26
10.	Maximum Power Spectral Density Feature, $\gamma_{max}$ . . . . .	27
11.	Expanded Plot: Maximum Power Spectral Density Feature, $\gamma_{max}$	28
12.	Absolute Phase Feature, $\sigma_{AP}$ . . . . .	28
13.	Expanded Plot: Absolute Phase Feature, $\sigma_{AP}$ . . . . .	29
14.	Direct Phase Feature, $\sigma_{DP}$ . . . . .	30
15.	Absolute Amplitude Feature, $\sigma_{AA}$ . . . . .	31
16.	Absolute Frequency Feature, $\sigma_{AF}$ . . . . .	31
17.	Expanded Plot: Absolute Frequency Feature, $\sigma_{AF}$ . . . . .	32
18.	Time Domain OFDM Waveform . . . . .	35
19.	DMRA Features for OFDM Waveform of Figure 18 . . . . .	36
20.	DMRA Absolute Phase Feature, $\sigma_{AP}$ , with OFDM Waveform Present . . . . .	37
21.	Expanded Plot: DMRA Absolute Phase Feature, $\sigma_{AP}$ , with OFDM Waveform Present . . . . .	38

Figure		Page
22.	DMRA Absolute Frequency Feature, $\sigma_{AF}$ , with OFDM Waveform Present . . . . .	39
23.	Decision Tree for the Modified DMRA . . . . .	39
24.	Decision Tree for the Modified DMRA (Limited to ASK, PSK, and OFDM) . . . . .	41
25.	Time Domain Waveforms for 4-ary Modulations . . . . .	46
26.	Normalized Centered Instantaneous Amplitude Response, $a_{cn}$ , for 4-ary Modulated Waveforms of Figure 25 . . . . .	46
27.	Normalized Centered Nonlinear Phase Response, $\phi_{NL}$ , for 4-ary Modulated Waveforms of Figure 25 . . . . .	47
28.	Nonlinear Phase Response, $\phi_{NL2}$ , for 4-ary Modulated Waveforms of Figure 25 . . . . .	47
29.	Normalized Centered Frequency Response, $f_N$ , for Binary Modulated Waveforms of Figure 25 . . . . .	48

## *List of Tables*

Table		Page
1.	Sample Confusion Matrix . . . . .	13
2.	Fundamental Modulation Signal Parameters . . . . .	15
3.	Spectral Weights for Gray Coded QAM-OFDM . . . . .	16
4.	RF Filter Bandwidths . . . . .	17
5.	Key Feature Threshold Values for Initial DMRA . . . . .	32
6.	Fundamental Modulation Confusion Matrix for $SNR = 10\text{ dB}$ and $BW = 6 \times r_s$ . . . . .	33
7.	Azzouz and Nandi's Confusion Matrix for $SNR = 10.0\text{ dB}$ [7] .	33
8.	Fundamental Modulation Confusion Matrix for $SNR = 11.0\text{ dB}$ and $BW = 6 \times r_s$ . . . . .	34
9.	Confusion Matrix for Unmodified DMRA with OFDM Input for $SNR = 11.0\text{ dB}$ and $BW = 6 \times r_s$ . . . . .	37
10.	Key Feature Threshold Values for the Modified DMRA . . . .	40
11.	Confusion Matrix with OFDM for $SNR = 11\text{ dB}$ and $BW = 6 \times r_s$	41
12.	Limited Confusion Matrix with OFDM for $SNR = 5.0\text{ dB}$ and $BW = 6 \times r_s$ . . . . .	42

# MODIFICATION OF A MODULATION RECOGNITION ALGORITHM TO ENABLE MULTI-CARRIER RECOGNITION

## I. Introduction

### 1.1 *Introduction*

Modulation recognition is important for both military and commercial communication applications, particularly in cases where enhanced situation awareness and/or channel assessment is required to mitigate intentional or collateral interference. Modulation recognition via template matching or statistical analysis is a key aspect of non-cooperative (non-matched filtering) signal interception, classification, and exploitation. The study of modulation type is important for several reasons. “First, applying the signal to an improper demodulator may partially or completely damage the content of the signal. Second, knowing the correct modulation type helps to recognize the threat and determine the suitable jamming waveform. Also, modulation recognition is important for national security.” [6]

### 1.2 *Problem Statement*

Orthogonal frequency division multiplexing (OFDM) is a multi-carrier technique that is becoming more prevalent as commercial companies migrate toward deployment of fourth generation (4G) communication systems. The advent of OFDM and its use in digital radio and cellular telephone systems indicates that a capability for distinguishing this modulation from fundamental modulations would be beneficial to the Air Force. This research focuses on developing a technique for the non-cooperative (non-matched filter) detection of OFDM signals by characterizing and modifying an existing automatic modulation recognition algorithm.

### ***1.3 Research Assumptions***

Several assumptions are made concerning the environment and the signals considered for this research. The channel is modelled with additive white Gaussian noise (AWGN). Input AWGN power levels are set to achieve desired signal-to-noise ratios (SNR) at the radio frequency (RF) filter output. Only one signal is present in the RF environment at a time, and it is assumed to be received along a direct line-of-sight path from the transmitter, i.e., no multi-path signal reflections are considered. With the exception of the OFDM signal itself, only binary and 4-ary fundamentally modulated waveforms are considered. The carrier frequency of all signals is set in the center of the RF filter. In all cases the symbol rate (symbols per second) and sampling frequency (samples per second) remain constant. Thus the actual bit rate (bits per second) varies as a function of modulation type, which dictates the number of bits per symbol.

### ***1.4 Research Scope***

The Digitally Modulated Signal Recognition Algorithm (DMRA), as developed by Azzouz and Nandi [7], is initially modelled here for the purpose of differentiating three fundamental modulated signal types: amplitude shift keying (ASK), phase shift keying (PSK), and frequency shift keying (FSK). Performance of the initial DMRA architecture is then characterized by introducing a quadrature amplitude modulated OFDM (QAM-OFDM) signal. Analysis of performance results is then conducted, and a modified DMRA architecture is proposed to permit reliable differentiation of OFDM from ASK, PSK, and FSK.

### ***1.5 Research Approach***

A literature search was conducted to determine the available types of modulation recognition algorithms and which had been used in the past. A 2003 modulation survey conducted by Su and Kosinski [18] provided a starting point. This survey introduced three types of algorithms which were classified as 1) baseband modulation

recognition, 2) almost baseband modulation recognition, and 3) direct modulation recognition. It also highlighted the work of Liedtke [16], DeSimio and Prescott [13,14], and Azzouz and Nandi [6–10], among others. Each of the algorithms is discussed further in Section 2.4.

As a result of this review and discussions with researchers at AFRL, the DMRA architecture offered by Azzouz and Nandi [7] was chosen for consideration. This choice was prudent given numerous citations in previous studies and a well documented implementation scheme. Thus the original DMRA architecture was developed in two research phases, a *development phase* which yielded key feature thresholds for the fundamental modulation types considered, and an *operational phase* which used the developmental thresholds and DMRA to establish recognition performance based on confusion matrices. Operational results from this work were then compared to Azzouz and Nandi’s [7] results to verify consistency.

Following development and operational characterization of the initial DMRA architecture, the QAM-OFDM waveform is introduced to determine the fundamental modulation type with which it would be most “confused”. Based on these results, a modified DMRA architecture is introduced to permit OFDM classification. The development process is then reproduced with the OFDM signal present to determine a new key feature and threshold. Operational performance results are then provided for the DMRA with the OFDM signal present.

## ***1.6 Materials and Equipment***

The modulated signals and DMRAs presented in this work were simulated using MATLAB® Version 7.0, developed by Mathworks, Inc. The simulations were run on a 2.2 GHz Athlon XP personal computer. This simulation methodology allowed precise control of the RF environment, signals, and key feature calculations.

## ***1.7 Thesis Organization***

Chapter 2 provides background information and analytic expressions for the modulations investigated, including amplitude shift keying (ASK), phase shift keying (PSK), frequency shift keying (FSK), and orthogonal frequency division multiplexing (OFDM). The DMRA architecture of Azzouz and Nandi [7] is also introduced. Chapter 3 presents the methodology used for conducting the research, including the parameters used to create the modulated signals and to calculate the key DMRA features. Chapter 4 provides simulation results and analysis for the fundamental modulation DMRA and the modified DMRA for recognizing OFDM. Chapter 5 presents conclusions drawn from the research and provides recommendations for possible future research. Additional supporting data is provided in the appendices.

## II. Background

### 2.1 Introduction

This chapter introduces signal characteristics for the modulation types considered and the digital signal modulation recognition algorithm that is used for estimating signal type. Section 2.2 describes the fundamental modulations (ASK, PSK, and FSK) and Section 2.3 introduces orthogonal frequency division multiplexing (OFDM). Section 2.4 provides a brief background on the use of modulation recognition. Section 2.5 describes the Digitally Modulated Signal Recognition Algorithm (DMRA) developed by Azzouz and Nandi [7]. Section 2.6 introduces the key features, classification process, and confusion matrices for the DMRA. Section 2.7 summarizes the chapter.

### 2.2 Signal Types: Fundamental Modulations

“Digital modulation is the process by which digital symbols are transformed into waveforms that are compatible with the characteristics of the channel.” [17] Bandpass modulation consists of converting an information signal into a sinusoidal waveform. This information can be conveyed in the following parameters of an RF carrier: amplitude, phase, frequency, or any combination thereof. The fundamental modulations, as described in this research, consist of modulations which only involve varying one signal parameter at a time on a symbol-by-symbol basis. The fundamental modulation types considered include amplitude shift keying (ASK), phase shift keying (PSK), and frequency shift keying (FSK).

*2.2.1 Amplitude Shift Keying (ASK).* Amplitude shift keying (ASK) is a form of amplitude modulation in which the modulating wave changes amplitude on a symbol-by-symbol basis using predetermined, discrete amplitude values. The analytic expression for M-ary ASK is

$$s_k(i) = a_k \cos \left( \frac{2\pi f_c i}{f_s} \right), \quad (1)$$

where  $f_c$  is the carrier frequency,  $a_k = A_k + A_o$  for  $A_o$  a constant bias factor,  $k = 1, 2, \dots, M$ , sample index  $i$  satisfies  $1 \leq i \leq N_s = f_s/r_s$ ,  $N_s$  is the number of samples per symbol,  $f_s$  is the sample frequency, and  $r_s$  is the symbol duration.

**2.2.2 Phase Shift Keying (PSK).** Phase shift keying (PSK) is “the form of phase modulation in which the modulating function shifts the instantaneous phase of the modulated wave on a symbol-by-symbol basis using predetermined, discrete phase values.” [11] The analytic expression for PSK is

$$s_k(i) = \sqrt{2P} \cos\left(\frac{2\pi f_c i}{f_s} + \phi_k\right), \quad (2)$$

where  $f_c$  is the carrier frequency,  $\phi_k = 2\pi k/M + \phi_o$ ,  $k = 0, 1, \dots, M-1$ , sample index  $i$  satisfies  $1 \leq i \leq N_s = f_s/r_s$ ,  $N_s$  is the number of samples per symbol,  $f_s$  is the sample frequency, and  $r_s$  is the symbol duration.

**2.2.3 Frequency Shift Keying (FSK).** Frequency shift keying (FSK) is “the form of frequency modulation in which the modulating wave shifts the output frequency on a symbol-by-symbol basis using predetermined values, and the output wave has no phase discontinuity.” [11] The analytic expression for FSK is

$$s_k(i) = \sqrt{2P} \cos\left(\frac{2\pi f_k i}{f_s}\right), \quad (3)$$

where  $f_c$  is the carrier frequency,  $f_k = f_c + kr_s$ , sample index  $i$  satisfies  $1 \leq i \leq N_s = f_s/r_s$ ,  $N_s$  is the number of samples per symbol,  $f_s$  is the sample frequency, and  $r_s$  is the symbol duration. The values of  $k$  are chosen as  $[\dots, -2, -1 < k < 1, 2, \dots]$ ,  $k \neq 0$ , to maintain a minimum FSK tone spacing of  $r_s$ .

### **2.3 Orthogonal Frequency Division Multiplexing (OFDM)**

Orthogonal Frequency Division Multiplexing (OFDM) is a combination of data modulation and multiple-access coding that segments a communication channel ac-

cording to frequency to permit channel sharing [1]. OFDM has been used since the mid-1960s and was originally patented in 1970 as a means to overcome the wasted bandwidth found in traditional frequency and time division multiplexing schemes [12]. At that time, the complexities associated with implementing OFDM made it too expensive for commercial applications. Thus, OFDM was primarily used for military applications until the 1990s.

Over the past ten years, the world of wireless communication has seen exponential growth. This growth has prompted the development of standards by the Institute of Electrical and Electronics Engineers (IEEE) for wireless devices for local area networks [15]. Although these standards implement various modulation types and coding schemes, including complementary code keying (CCK) and packet binary convolutional coding (PBCC), the predominant modulation cited in the IEEE 802.11a, 802.11g, 802.16a, and 802.15.3a(proposed) standards is OFDM [2–5].

OFDM is a combination of modulation and multiplexing that relies on spectral segmentation to provide signal discrimination / separability, i.e., it divides the spectrum into a number of equally spaced regions where mutually orthogonal data modulated tones are placed. The instantaneous spectrum of these tones, which are independently modulated with user data, do overlap, yet they do so while providing manageable interference with each other.

The time domain representation for the  $k^{th}$  quadrature amplitude modulated OFDM (QAM-OFDM) symbol comprised of  $N_c$  total subcarriers per symbol, or  $2N_c$  total bits per symbol given that there are two bits per QAM symbol, is

$$s_k(t) = \sum_{n=1}^{N_c} \{B_c(n) \cos(2\pi f_n t) + B_s(n) \sin(2\pi f_n t)\}, \quad (4)$$

where  $f_n$  is the  $n^{th}$  subcarrier frequency and  $B_c(n)$  and  $B_s(n)$  are data dependent *cosine* and *sine* weights, respectively, for the  $n^{th}$  subcarrier given by

$$B_c(n) = (-1)^{b_{k+2(n-1)}} \quad B_s(n) = (-1)^{b_{k+(2n-1)}} \quad (5)$$

for an input sequence of bits for the  $k^{th}$  QAM-OFDM symbol given by

$$B_k = [b_1, b_2, b_3, \dots b_{2N_c}]. \quad (6)$$

The resultant frequency domain expression for the QAM-OFDM symbol given by Equation 4 is

$$S_k(f) = \sum_{n=1}^{N_c} \left[ \frac{1}{2} \{B_{Pos}\} \delta(f - f_n) + \frac{1}{2} \{B_{Neg}\} \delta(f + f_n) \right], \quad (7)$$

where the complex ( $j$  used to denote  $\sqrt{-1}$  here) positive and negative frequency components are

$$B_{Pos}(n) = B_c(n) - jB_s(n) \quad B_{Neg}(n) = B_c(n) + jB_s(n). \quad (8)$$

## 2.4 Modulation Recognition

One of the earlier reports published on the subject of automatic classification of modulation was written by Weaver, Cole, Krumland, and Miller [19]. This technical report, written for the Air Force Avionics Laboratory, focused on the rapid and automatic identification of modulation types of high frequency radio signals. In 1984, Liedtke [16] focused on the real-time classification of ASK2, FSK2, PSK2, PSK4, and PSK8 modulations. His procedure used a universal demodulator for feature extraction. DeSimio and Prescott [13, 14] later introduced, in 1988, a procedure to classify ASK2, PSK2, PSK4, and FSK2 using moment analysis. Subsequent to this earlier work, Azzouz and Nandi [6–10] developed multiple procedures for the classification of ASK2, ASK4, PSK2, PSK4, FSK2, and FSK4. Their classical decision theoretic methods are discussed in Section 2.5.

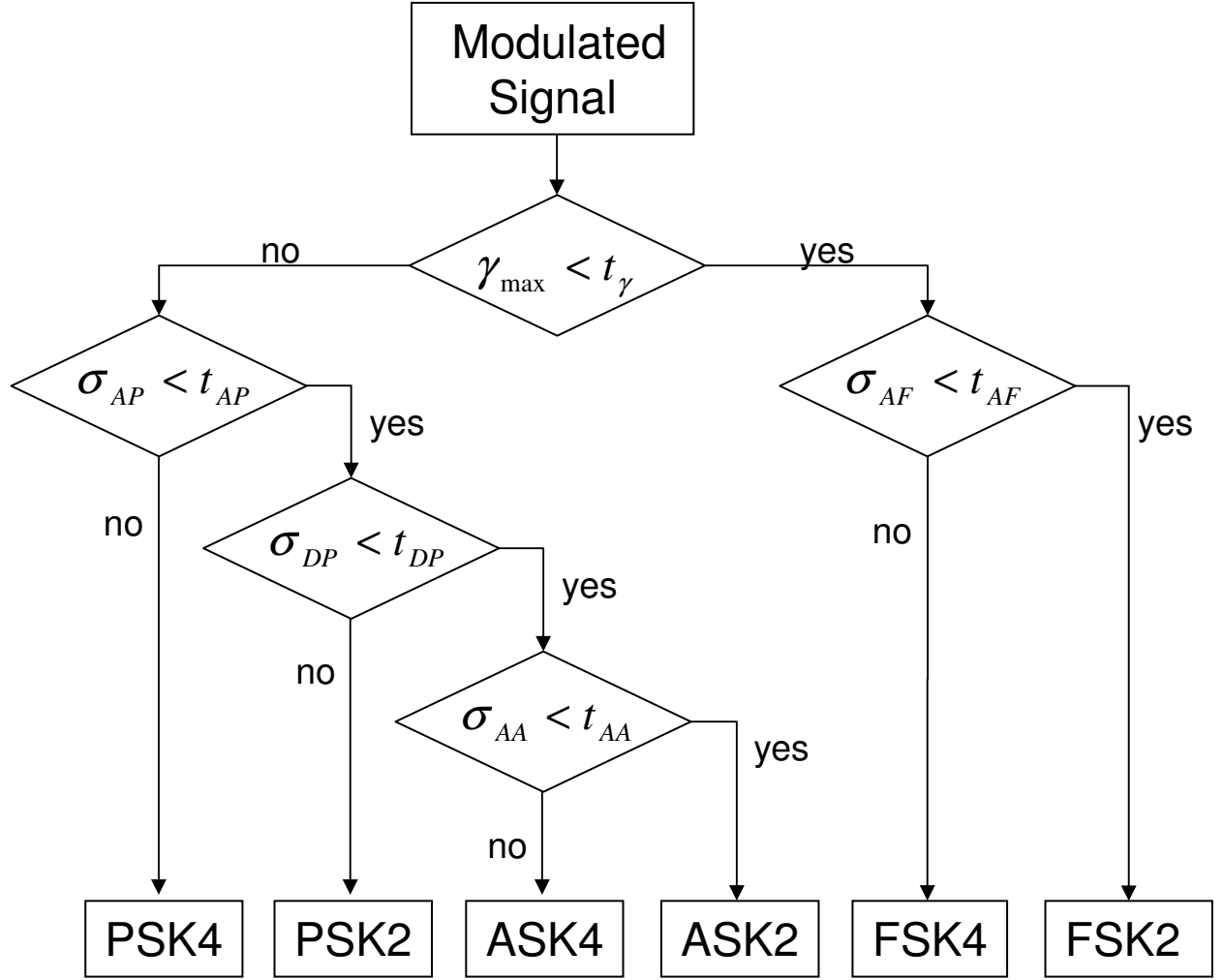


Figure 1: Fundamental Modulation DMRA Decision Tree [7]

### 2.5 Digitally Modulated Signal Recognition Algorithm (DMRA)

The digitally modulated signal recognition algorithm (DMRA) considered for this research was developed by Azzouz and Nandi [7] and utilizes a decision-theoretic approach. Each decision about modulation type is derived from information extracted across the entire observation interval, rather than on a symbol-by-symbol basis. The final decision is based on the calculation of five key features which are extracted from the instantaneous amplitude, phase, and frequency of the signal. A decision threshold for each of these features is set to discriminate between modulations. The fundamental modulation DMRA decision tree is outlined in Figure 1.

## 2.6 Key Feature Extraction

The DMRA recognition performance is based on five key features:  $\gamma_{max}$ ,  $\sigma_{AP}$ ,  $\sigma_{DP}$ ,  $\sigma_{AA}$ , and  $\sigma_{AF}$ . This section describes the calculation of each key feature as introduced by Azzouz and Nandi [7].

**2.6.1 Maximum Power Spectral Density Feature ( $\gamma_{max}$ ).** The first key feature shown in Figure 1,  $\gamma_{max}$ , separates the signals that contain amplitude information (ASK2, ASK4, PSK2, and PSK4) from those signals that do not have amplitude information (FSK2 and FSK4). It denotes the *maximum power spectral density* of the normalized centered instantaneous amplitude of the intercepted signal and is [7]

$$\gamma_{max} = \frac{\max |DFT(a_{cn}(i))|^2}{N_s}, \quad (9)$$

where  $N_s$  is the number of samples per segment and  $a_{cn}(i)$ , the *normalized centered instantaneous amplitude*, is [7]

$$a_{cn}(i) = \frac{a(i)}{m_a} - 1 \quad (10)$$

for  $m_a$ , the average value of instantaneous amplitude, given by [7]

$$m_a = \frac{1}{N_s} \sum_{i=1}^{N_s} a(i), \quad (11)$$

where  $a(i)$  is the *instantaneous amplitude* of the signal.

**2.6.2 Absolute Phase Feature ( $\sigma_{AP}$ ).** The second key feature shown in Figure 1,  $\sigma_{AP}$ , separates the signal that contains absolute phase information (PSK4) from those signals that have no absolute phase information (ASK2, ASK4, and PSK2). It denotes the standard deviation of the *absolute values of the centered non-linear component of the instantaneous phase* evaluated over the non-weak intervals of a

signal segment and is [7]

$$\sigma_{AP} = \sqrt{\frac{1}{C} \left( \sum_{a_n(i) > a_t} \phi_{NL}^2(i) \right) - \left( \frac{1}{C} \sum_{a_n(i) > a_t} |\phi_{NL}(i)| \right)^2}, \quad (12)$$

where  $\phi_{NL}(i)$  is the values of the centered non-linear component of the *instantaneous phase*  $\phi(i)$  and  $C$  is the number of samples in  $\phi_{NL}(i)$  for which the amplitude  $a_n(i)$  is above a threshold,  $a_t$ . This threshold is used to enhance algorithm performance by eliminating portions of the signal that are most affected by noise and is considered to remove the “weak” intervals of a signal segment.

**2.6.3 Direct Phase ( $\sigma_{DP}$ ).** The third key feature shown in Figure 1,  $\sigma_{DP}$ , separates the signal that contains direct phase information (PSK2) from those signals that have no direct phase information (ASK2 and ASK4). It denotes the standard deviation of the centered non-linear component of the *direct (non-absolute) instantaneous phase*, evaluated over the non-weak intervals of a signal segment and is [7]

$$\sigma_{DP} = \sqrt{\frac{1}{C} \left( \sum_{a_n(i) > a_t} \phi_{NL}^2(i) \right) - \left( \frac{1}{C} \sum_{a_n(i) > a_t} \phi_{NL}(i) \right)^2}. \quad (13)$$

**2.6.4 Absolute Amplitude ( $\sigma_{AA}$ ).** The fourth key feature shown in Figure 1,  $\sigma_{AA}$ , separates the signal that has absolute and direct amplitude information (ASK4) from the signal that has no absolute amplitude information (ASK2). It denotes the standard deviation of the *absolute values of the normalized-centered instantaneous amplitude* of a signal segment and is [7]

$$\sigma_{AA} = \sqrt{\frac{1}{N_s} \left( \sum_{i=1}^{N_s} a_{cn}^2(i) \right) - \left( \frac{1}{N_s} \sum_{i=1}^{N_s} |a_{cn}(i)| \right)^2}. \quad (14)$$

*2.6.5 Absolute Frequency ( $\sigma_{AF}$ ).* The fifth key feature shown in Figure 1,  $\sigma_{AF}$ , separates the signal that has no absolute frequency information (FSK2) from the signal that has absolute and direct frequency information (FSK4). It denotes the standard deviation of the *absolute value of the normalized-centered instantaneous frequency* evaluated over the non-weak intervals of a signal segment and is [7]

$$\sigma_{AF} = \sqrt{\frac{1}{C} \left( \sum_{a_n(i) > a_t} f_N^2(i) \right) - \left( \frac{1}{C} \sum_{a_n(i) > a_t} |f_N(i)| \right)^2}, \quad (15)$$

where

$$f_N(i) = \frac{f(i) - m_f}{r_s}. \quad (16)$$

Here  $r_s$  is the symbol rate of the sequence and  $m_f$ , the average value of the instantaneous frequency, is given by [7]

$$m_f = \frac{1}{N_s} \sum_{i=1}^{N_s} f(i), \quad (17)$$

where  $f(i)$  is the *instantaneous frequency* of the signal.

*2.6.6 Classification.* Signal classification (recognition) is based on reliably measuring the signal parameters and calculating the signal features. These signal features are then compared to set thresholds,  $t_\gamma$ ,  $t_{AP}$ ,  $t_{DP}$ ,  $t_{AA}$ , and  $t_{AF}$ . Various algorithms can be created using the five key signal features by varying the order that thresholds are applied and decisions are made. The algorithm selected for this research is the DMRA I architecture as previously shown in Figure 1 [7].

*2.6.7 Confusion Matrices.* The confusion matrix is used to show DMRA performance results in a table format. The first column of entries contains the modulation types that are input into the DMRA. The entries in the first row represent the modulation types of signal classification. For illustrative purposes, a sample confusion matrix for 200 input signal replications is shown in Table 1. In this case, the matrix

Table 1: Sample Confusion Matrix

Simulated Modulation Type	Deduced Modulation Type		
	Mod. 1	Mod. 2	Mod. 3
Modulation 1	140	60	0
Modulation 2	0	200	0
Modulation 3	1	0	199

shows that the success rate for classifying Modulation 2 is 100% and that Modulation 1 is confused 30% of the time with Modulation 2 (60 occurrences). Modulation 3 is successfully classified 99.5% of the time, with only one occurrence confused with Modulation 1.

## 2.7 Summary

This chapter introduced the signal modulation characteristics for the fundamental modulation types of ASK, PSK, and FSK and the more complex OFDM structure. The DMRA used for initial results was introduced, including the analytic expressions for each of the five key features required. The fundamental modulation DMRA decision tree was presented to illustrate the signal classification process. Finally, the confusion matrix was introduced as a means for presenting recognition data. Chapter 3 provides the methodology and specific details used for implementing the DMRA process.

### III. Methodology

#### 3.1 Introduction

Performance of the DMRA process described in Chapter 2 and shown in Figure 1 is determined by comparing key features to set thresholds. The first step in expanding the DMRA architecture to include OFDM recognition capability is to verify consistency with the DMRA model presented by Azzouz and Nandi [7]. Figure 2 shows the process used here to determine key feature threshold values.

The purpose and functionality of each block in Figure 2 is addressed in this chapter. Section 3.2 and Section 3.3 discuss characteristics of the fundamental modulations and the OFDM signals. Section 3.4 provides details of the RF bandpass filter and calculations used to determine output signal-to-noise ratio (SNR). Section 3.5 and Section 3.6 outline the signal parameters and the calculation of the five key features. Section 3.7 considers *developmental* procedures and *operational* performance of the DMRA. Section 3.8 describes OFDM signal introduction into the DMRA. Finally, Section 3.9 summarizes the chapter.

#### 3.2 Modulated Signals: Fundamental Modulation Parameters

All signals,  $s_k(i)$ , used in the simulations are generated over one observation interval using the analytic expressions of Chapter 2 and parameters consistent with those of [7].

The following parameter values are used in simulation:

- Carrier Frequency,  $f_c = 150 \text{ kHz}$
- Sampling Rate,  $f_s = 1200 \text{ kHz}$
- Symbol Rate,  $r_s = 12.5 \text{ kHz}$
- Number of Samples per Symbol Duration,  $N_s = 96$
- Observation Interval,  $T_{obs} = 20 \text{ Symbols} = 1920 \text{ Samples}$

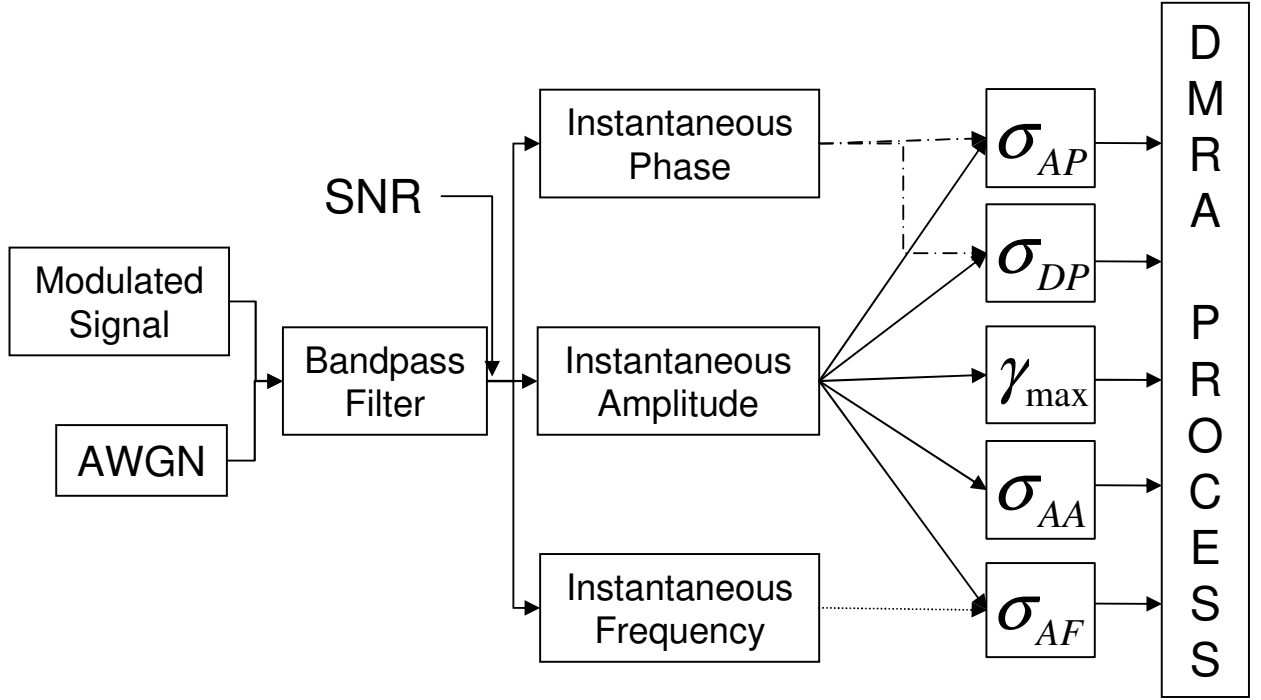


Figure 2: Modulation Recognition Process

The  $k^{th}$  symbol of the fundamental modulations is generated using

$$s_k(i) = a_k \cos \left( \frac{2\pi f_k i}{f_s} + \phi_k \right), \quad (18)$$

where the amplitude ( $a_k$ ), frequency ( $f_k$ ) and phase ( $\phi_k$ ) are given in Table 2.

Table 2: Fundamental Modulation Signal Parameters

Modulation Type	$a_k$	$f_k$ (kHz)	$\phi_k$
ASK2	$.9k + .1$	$f_c$	0
ASK4	$.3214k + .0357$	$f_c$	0
PSK2	1	$f_c$	$(1 - k)\pi$
PSK4	1	$f_c$	$k\frac{\pi}{2}$
FSK2	1	$4r_s k + f_c - 2r_s$	0
FSK4	1	$f_c - (k + 1)r_s$ if $k < 2$ $f_c + (k - 1)r_s$ if $k \geq 2$	0

Table 3: Spectral Weights for Gray Coded QAM-OFDM

Bit Pattern	$B_{Pos}$	$B_{Neg}$
0 0	$1 - i$	$1 + i$
1 0	$-1 - i$	$-1 + i$
0 1	$1 + i$	$1 - i$
1 1	$-1 + i$	$-1 - i$

### 3.3 Modulated Signals: OFDM

The  $k^{th}$  symbol of the 4-ary, QAM-OFDM is generated by taking the Inverse Fast Fourier Transform (IFFT) of

$$S_k(f) = \sum_{n=1}^{N_c} \left[ \frac{1}{2} \{B_{Pos}\} \delta(f - f_n) + \frac{1}{2} \{B_{Neg}\} \delta(f + f_n) \right], \quad (19)$$

where for Gray Coded QAM the  $B_{Pos}$  and  $B_{Neg}$  values of Table 3 are used. The following parameter values are used in QAM-OFDM simulations:

- Number of Carriers used per OFDM Symbol,  $N_{car} = 5$
- Number of OFDM Symbols Generated,  $T_{obs} = 20$
- Number of Frequency Components (IFFT Points),  $N_S = 96$
- Center Frequency Component,  $f_c = 150 \text{ kHz}$
- Symbol Rate,  $r_s = 12.5 \text{ kHz}$

### 3.4 Bandpass Filter Characteristics and SNR Calculation

An 8<sup>th</sup>-order Chebyshev bandpass filter having a 0.001 dB bandpass ripple was simulated for each signal considered. The RF filter bandwidth used for each signal is outlined in Table 4. “In practice, the bandwidth of any intercepting receiver is chosen to be slightly larger than the intercepted signal bandwidth” [7]. Therefore, the simulated noise is bandlimited to a  $-3.0 \text{ dB}$  bandwidth of 1.16 times the simulated modulated signal bandwidth. The simulated Chebyshev filter responses for the bandwidths listed in Table 4 are shown in Figure 3.

Table 4: RF Filter Bandwidths

Modulation Type	Theoretical Expression	Simulated Value (kHz)
ASK	$4r_s$	50
PSK	$6r_s$	75
FSK	$8r_s$	100
OFDM	$5r_s$	62.5

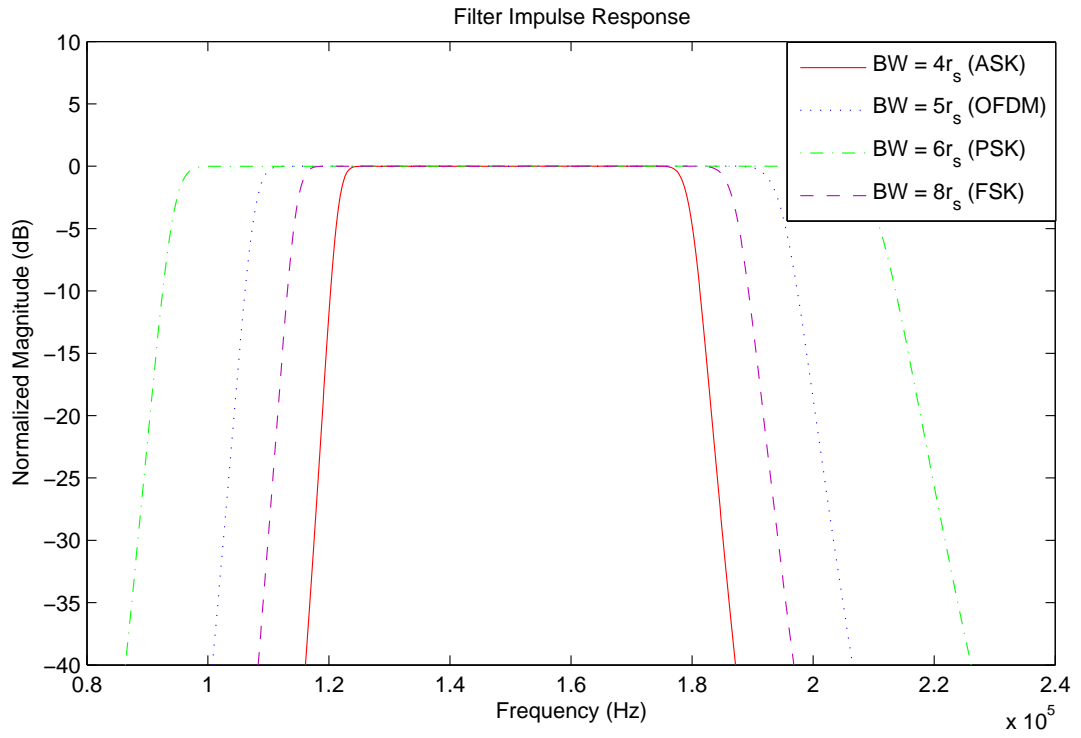


Figure 3: Filter Response of 8<sup>th</sup>-Order Chebyshev Filter

The signal-to-noise ratio (SNR) for each input signal is adjusted at the bandpass filter output. The input noise  $n(t)$  is generated using a zero-mean normally distributed random number generator and is filtered at the same bandwidth as the modulated signal. To establish the desired SNR at the filter output, the sampled input noise sequence is multiplied by a scale factor [7]

$$R_{sn} = \sqrt{\frac{S_p}{N_p}} \left( 10^{\frac{-SNR}{20}} \right), \quad (20)$$

where  $SNR$  is calculated in decibels,  $S_p = \frac{1}{N} \sum_{i=1}^N s^2(i)$ , and  $N_p = \frac{1}{N} \sum_{i=1}^N n^2(i)$ .

### 3.5 *Signal Qualifying Parameters*

The three signal qualifying parameters used for calculating the key features, include instantaneous amplitude, instantaneous phase, and instantaneous frequency. Instantaneous amplitude  $a(i)$  is calculated by taking the absolute value of the Hilbert transform of the signal. Instantaneous phase  $\phi(i)$  is calculated by taking the arc tangent of the imaginary part of the Hilbert transform divided by the real part of the Hilbert transform. Instantaneous frequency  $f(i)$  is calculated by taking the derivative of the instantaneous phase.

### 3.6 *Key Feature Extraction*

Analytic expressions for each of the key features are outlined in Section 2.4. For all results presented a normalized amplitude threshold  $a_t = 1$  was used.

### 3.7 *DMRA Processing*

Characterization of the DMRA process used for signal classification involved two phases of research. In the first *developmental* phase, signals with known modulations are input into the system and used to calculate key feature values for a range of desired SNR values. The features values are then plotted versus SNR to establish thresholds for the decision tree of Figure 1. In the second *operational* phase, signals

of interest are input to the DMRA, which is tasked with automatically deciding which modulation type is present using the thresholds calculated in the development stage.

*3.7.1 DMRA Development for Fundamental Modulations.* The *development* phase determines the following five key feature thresholds,  $t_\gamma$ ,  $t_{AP}$ ,  $t_{DP}$ ,  $t_{AA}$ , and  $t_{AF}$ , with threshold determination based on 400 realizations (observation intervals) for each of the six fundamental modulated signals (binary and 4-ary signaling for each fundamental modulation type). These realizations are calculated for SNR values ranging from 0.0 to 20.0 dB. Note that during the *development* phase, the RF filter bandwidth is changed to “match” (correspond) the approximate null-to-null bandwidth of the input signal as given in Table 4.

Figure 4 shows a sample key feature plot for illustrating the threshold determination process. In this instance separation between Signals 1 & 2 and Signal 3 is desired. It can be seen that the threshold value needed to separate these signals is 6 and is valid for  $SNR \geq 0$  dB.

*3.7.2 DMRA Operation for Fundamental Modulations.* The *operational* phase implements the initial DMRA architecture using the thresholds calculated in the development phase. Each of the fundamental modulations is simulated for 400 realizations (observation intervals) using random data. Each of these simulations is run for a given SNR value. During this phase, the RF filter bandwidth is *fixed* for all input signal types at a value of  $6 \times r_s$ . This bandwidth is chosen because it is the narrowest bandwidth that equals the maximum null-to-null bandwidth of the fundamental signals considered, specifically the FSK4 signal. Operational DMRA simulation results are summarized using a confusion matrix as described in Section 2.6.7. These confusion matrices are then compared to the confusion matrices created by Azzouz and Nandi [7] to verify consistency.

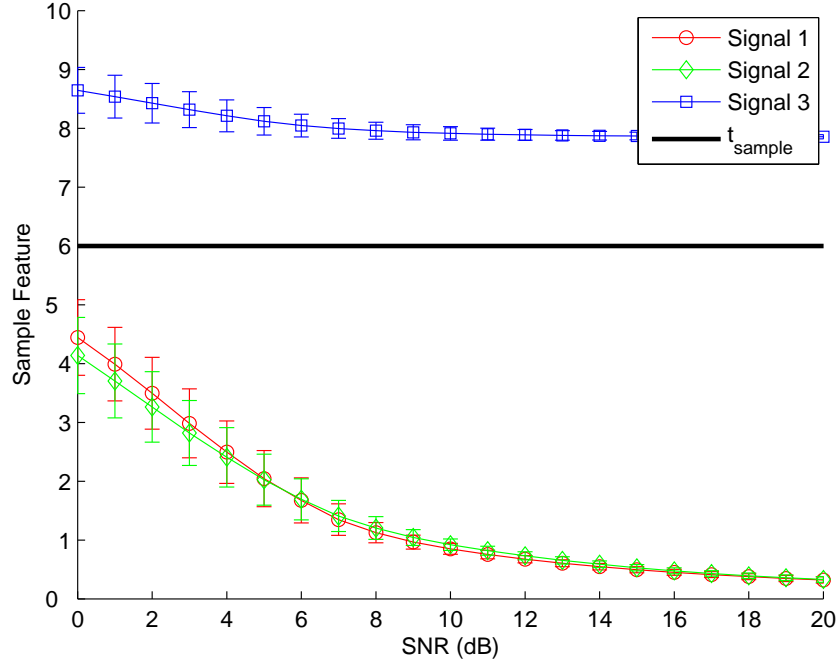


Figure 4: Sample Feature Threshold Determination

### 3.8 Introduction of OFDM into DMRA

To determine how to adjust the original DMRA architecture to include OFDM decision criteria, it is necessary to determine how OFDM is classified in the original DMRA. This determination is accomplished by introducing the OFDM waveform into original DMRA without changing the feature thresholds, SNR value, or RF filter bandwidth. Using the data presented in this confusion matrix, it can be determined which features or thresholds need to be adjusted for classifying OFDM. Once the new features or thresholds are determined, they are compared to see which DMRA modification provides the best performance at lower SNR values. The modified DMRA is then used to create new confusion matrices for the performance of OFDM.

### 3.9 Summary

This chapter introduced and outlined the modulation recognition process shown in Figure 2. The modulation types (ASK, PSK, FSK, and OFDM), filter charac-

teristics, and SNR realizations were discussed. The methodology for implementing the original DMRA architecture was presented, as well as a process for characterizing DMRA performance with an OFDM signal present. Operational results for the DMRA and modified DMRA are shown in Chapter 4.

## IV. Results and Analysis

### 4.1 Introduction

This chapter provides developmental and operational performance results for the Digitally Modulated Signal Recognition Algorithm (DMRA) introduced in Chapters 2 and 3. First, Section 4.2 provides the time waveforms and instantaneous detection results which are used in the initial DMRA architecture. Next, Section 4.3 presents the key feature plots and thresholds for the fundamental modulations. Section 4.4 provides the operational results and analysis for the fundamental modulations. Then Section 4.5 introduces the OFDM waveform and provides performance results for the initial DMRA architecture with the OFDM waveform present. Results are then presented for a modified DMRA architecture, which includes an additional key feature decision for recognizing OFDM.

### 4.2 Fundamental Modulation Time Waveforms

The fundamental waveforms are modulated using Equation 18 with the signal parameters listed in Table 2. The results shown in this section are for the binary modulations. Additional results for the 4-ary modulations are presented in Appendix A.

Figure 5 shows representative time domain waveforms for one observation interval,  $T_{obs}$ , consisting of 20 symbols. Results shown in this figure, and subsequent results in Figure 6 through Figure 9, were generated using a random binary waveform. The random binary waveform shown in the following figures is given by: [10101100101111001000].

*4.2.1 Normalized Centered Amplitude Response ( $a_{cn}$ ).* The normalized centered amplitude response,  $a_{cn}$ , is used in the calculation of  $\gamma_{max}$  and  $\sigma_{AP}$  for the DMRA. Equation 10 gives the expression for calculating  $a_{cn}$ . Figure 6 shows  $a_{cn}$  responses corresponding to the ASK2, PSK2, and FSK2 time domain waveforms of Figure 5. With the exception of some minuscule spurious responses occurring at

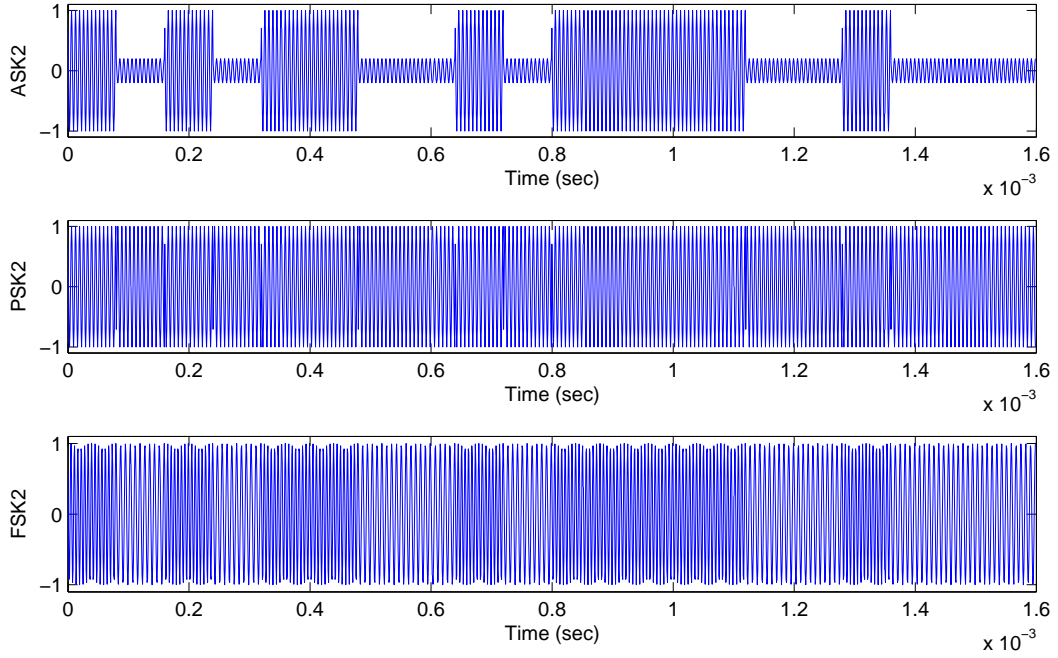


Figure 5: Time Domain Waveforms for Binary Modulations

symbol boundaries in the PSK2 and FSK2  $a_{cn}$  responses, the ASK2  $a_{cn}$  response is the only response reflecting structure which is consistent with the modulation type employed.

*4.2.2 Normalized Centered Nonlinear Phase Response ( $\phi_{NL}$ ).* The normalized centered nonlinear phase response,  $\phi_{NL}$ , is used in the calculation of  $\sigma_{AP}$  and  $\sigma_{DP}$  for the DMRA. In first calculating  $\phi_{NL}$  the signal phase is limited to values between  $-\pi$  and  $\pi$ . As shown in Figure 7, only the PSK2  $\phi_{NL}$  response accurately reflects structure which is consistent with the modulation type employed. The ASK2  $\phi_{NL}$  response reflects minor variation near symbol boundaries and the FSK2  $\phi_{NL}$  response, if viewed unwrapped, would reflect a linear phase progression within each symbol interval, which is consistent with constant tone transmission.

*4.2.3 Normalized Centered Frequency Response ( $f_N$ ).* The normalized centered frequency response,  $f_N$ , is used in the calculation of  $\sigma_{AF}$  for the DMRA. The

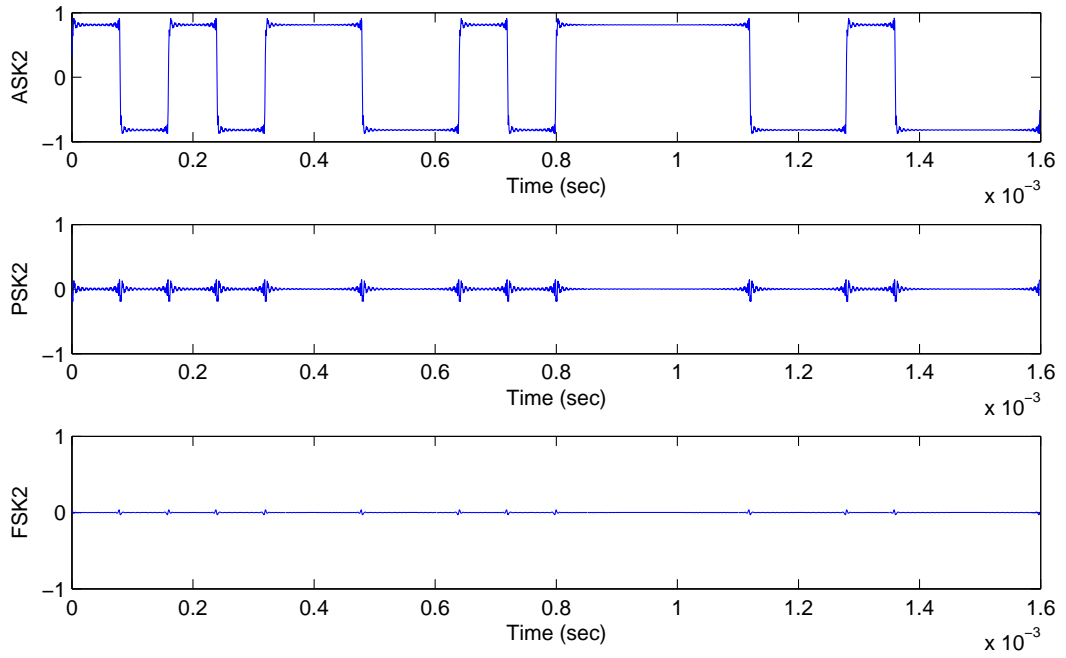


Figure 6: Normalized Centered Instantaneous Amplitude Response,  $a_{cn}$ , for Binary Modulated Waveforms of Figure 5

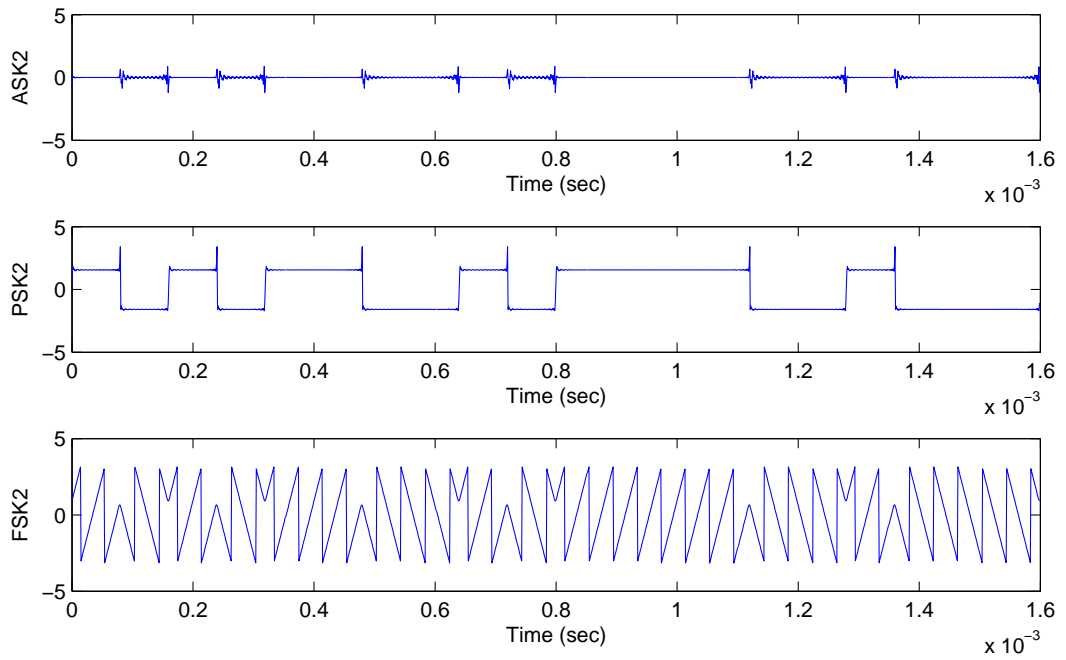


Figure 7: Normalized Centered Nonlinear Phase Response,  $\phi_{NL}$ , for Binary Modulated Waveforms of Figure 5

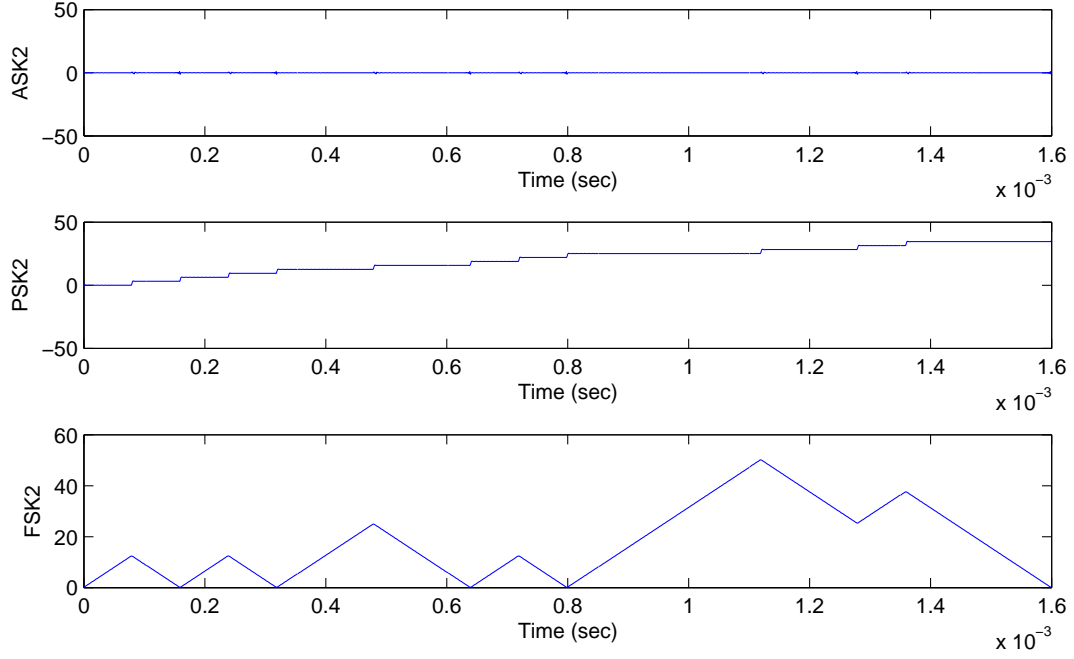


Figure 8: Nonlinear Phase Response,  $\phi_{NL2}$ , for Binary Modulated Waveforms of Figure 5

analytic expression for calculating  $f_N$  is given in Equation 16. To calculate the  $f_N$  response, the instantaneous frequency,  $f(i)$  is first calculated. As indicated in Chapter 3, instantaneous frequency  $f(i)$  is given as the derivative of instantaneous phase. To accurately determine the frequency, the absolute phase values must be used versus the modulo phase values of  $\phi_{NL}$  shown in Figure 7. Therefore, a non-modulo phase function,  $\phi_{NL2}$ , is used as shown in Figure 8. Using  $\phi_{NL2}$ , the normalized centered frequency responses  $f_N$  of the time domain waveforms in Figure 5 are obtained as shown in Figure 9. With the exception of spurious responses appearing in the ASK2 and PSK2 plots, the  $f_N$  response for FSK2 is the only plot showing structure which is consistent with the modulation type employed.

### 4.3 Initial DMRA Development for Fundamental Modulations

The initial DMRA development for fundamental modulations begins by first determining threshold values for the five key DMRA features. Each plot in this

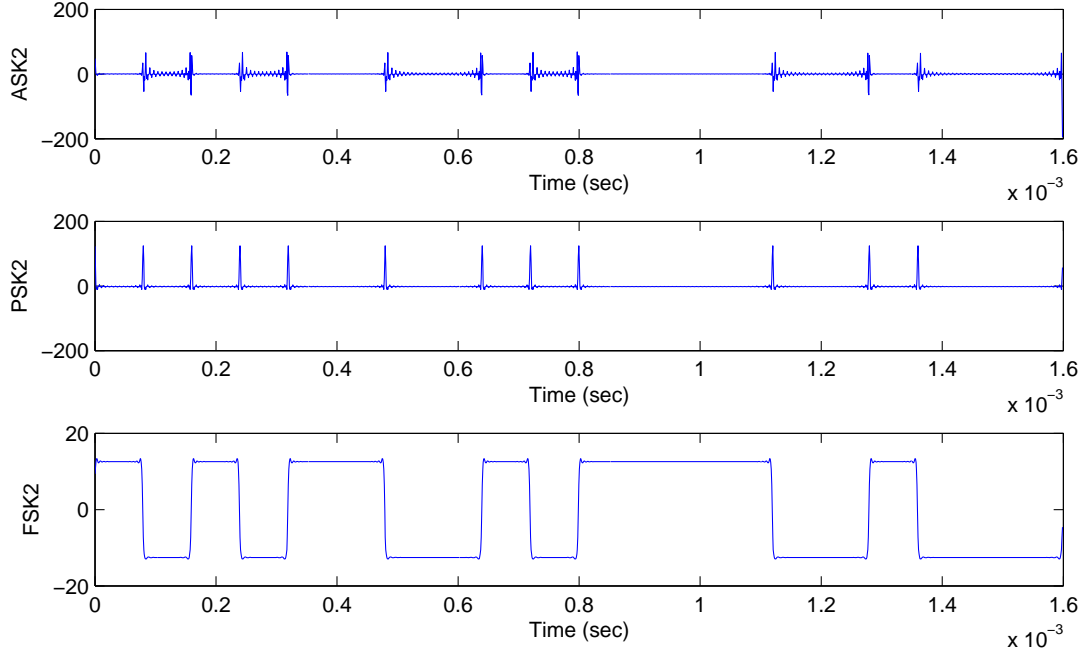


Figure 9: Normalized Centered Frequency Response,  $f_N$ , for Binary Modulated Waveforms of Figure 5

section is derived using 400 realizations and SNR values ranging from 0.0 to 20.0 dB. The error bars contained in each plot represent one standard deviation from the mean value.

*4.3.1 Dependence of  $\gamma_{max}$  on SNR.* The first key feature,  $\gamma_{max}$ , is calculated for all six fundamental modulations (ASK2, ASK4, PSK2, PSK4, FSK2, FSK4). Since FSK2 and FSK4 have a constant instantaneous amplitude, their normalized centered instantaneous amplitude response  $a_{cn}$  is ideally zero. [7]. In practice, however, a near-zero response similar to that shown in Figure 6 for FSK2 is achieved. Thus, the initial DMRA architecture first divides signals into two groups, those exhibiting some instantaneous amplitude response (ASK2, ASK4, PSK2, PSK4) and those having no amplitude response (FSK2, FSK4). Results for 400 realizations are presented in Figure 10, with Figure 11 providing an expanded view. As shown in Figure 11 by the solid horizontal line, a DMRA threshold value for  $\gamma_{max}$  of  $t_\gamma = 2.32$  is chosen. For this threshold value, there is at least one standard deviation of separability for  $SNR \geq$

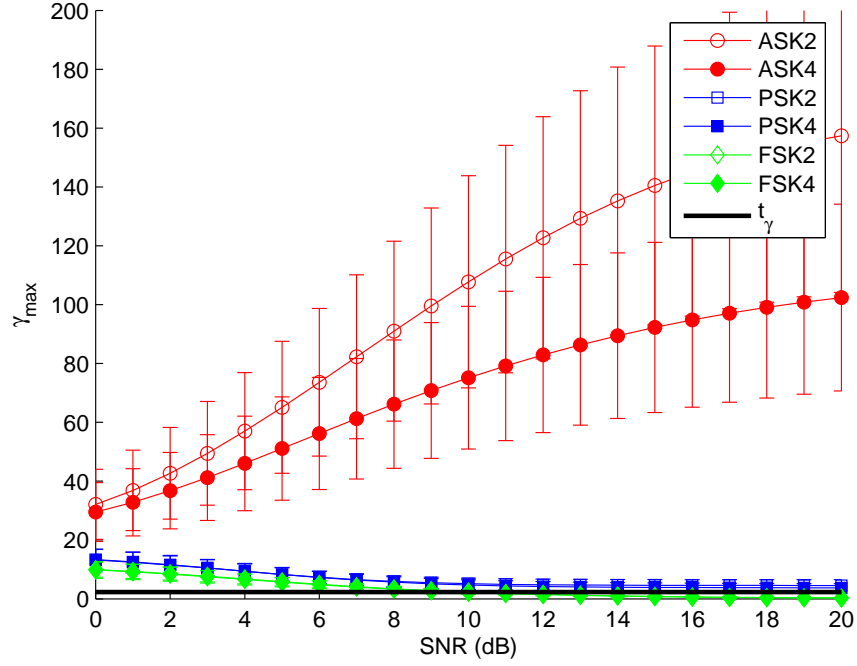


Figure 10: Maximum Power Spectral Density Feature,  $\gamma_{max}$

11.0 dB. Note also that for this threshold value and all SNR values considered, the  $\gamma_{max}$  value for signals possessing an instantaneous amplitude response (ASK2, ASK4, PSK2, PSK4) remain above the threshold.

*4.3.2 Dependence of  $\sigma_{AP}$  on SNR, ( $\gamma_{max} \geq t_{\gamma}$ ).* The second key feature considered is  $\sigma_{AP}$ , which is calculated for the four modulations containing instantaneous amplitude information (ASK2, ASK4, PSK2, PSK4). Since ASK2, ASK4, and PSK2 have no absolute phase information, they can be separated from PSK4, which contains absolute phase information. Results for 400 realizations are presented in Figure 12, with Figure 13 providing an expanded view. As shown in Figure 13 by the solid horizontal line, a DMRA threshold value for  $\sigma_{AP}$  of  $t_{AP} = 0.77$  is chosen. For this threshold value, there is at least one standard deviation of separability for  $SNR \geq 0.0$  dB.

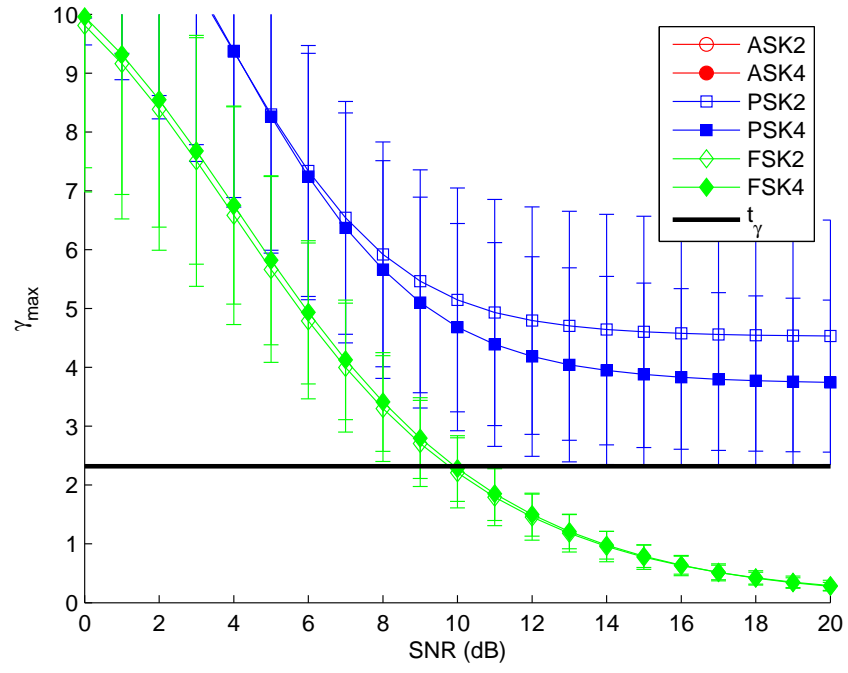


Figure 11: Expanded Plot: Maximum Power Spectral Density Feature,  $\gamma_{max}$

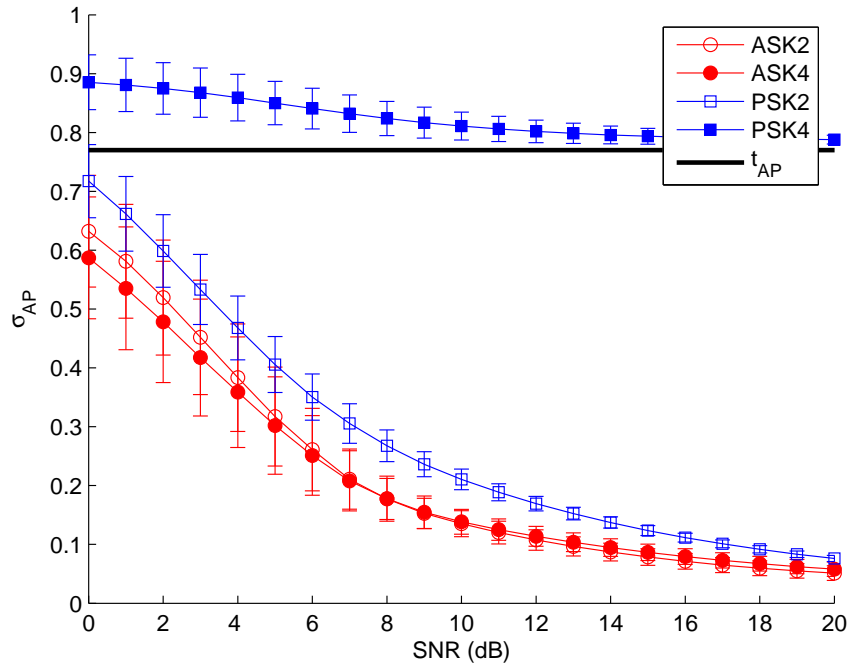


Figure 12: Absolute Phase Feature,  $\sigma_{AP}$

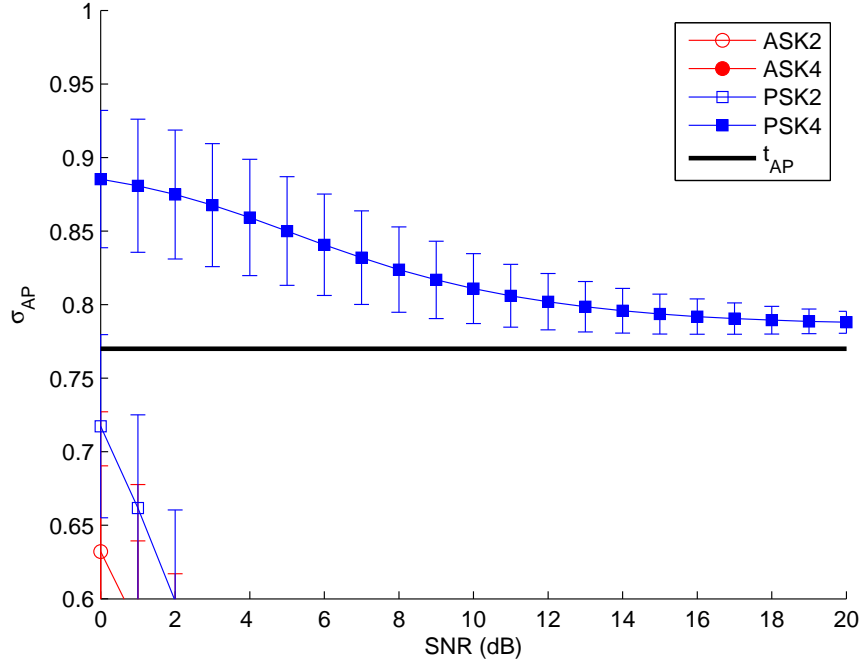


Figure 13: Expanded Plot: Absolute Phase Feature,  $\sigma_{AP}$

*4.3.3 Dependence of  $\sigma_{DP}$  on SNR, ( $\sigma_{AP} \leq t_{AP}$ ).* The third key feature considered is  $\sigma_{DP}$ , which is calculated for the three modulations not containing absolute phase information (ASK2, ASK4, PSK2). Since ASK2 and ASK4 have no direct phase information, they can be separated from PSK4 which contains direct phase information. Results for 400 realizations are presented in Figure 14. As shown in Figure 14 by the solid horizontal line, a DMRA threshold value for  $\sigma_{DP}$  of  $t_{DP} = 1.2$  is chosen. For this threshold value, there is at least one standard deviation of separability for  $SNR \geq 0.0$  dB.

*4.3.4 Dependence of  $\sigma_{AA}$  on SNR, ( $\sigma_{DP} \leq t_{DP}$ ).* The fourth key feature considered is  $\sigma_{AA}$ , which is calculated for the two modulations not containing direct phase information (ASK2 and ASK4). Since ASK2 has no absolute amplitude information, it can be separated from ASK4 which contains absolute amplitude information. Results for 400 realizations are presented Figure 15. As shown in Figure 15 by the solid horizontal line, a DMRA threshold value for  $\sigma_{AA}$  of  $t_{AA} = 0.283$  is chosen.

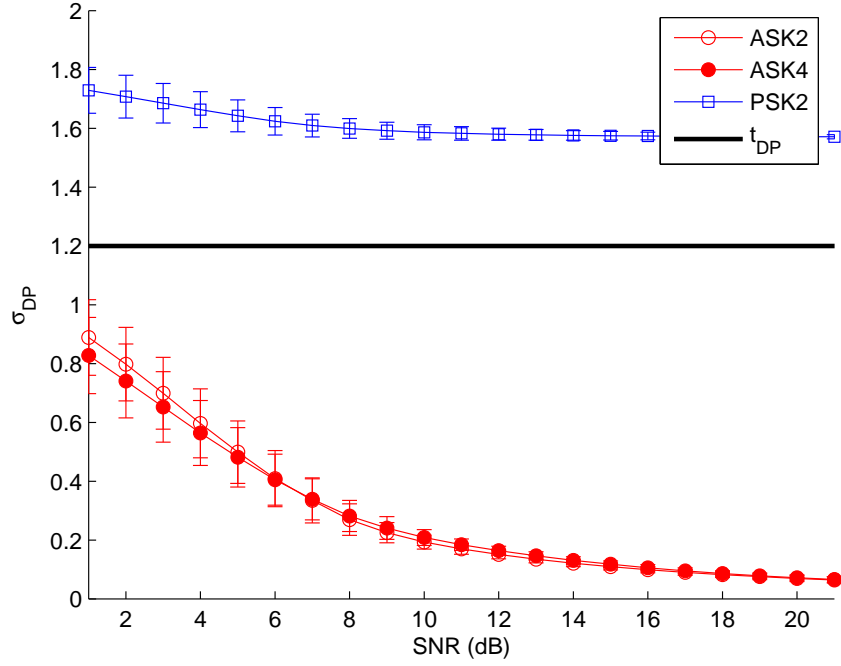


Figure 14: Direct Phase Feature,  $\sigma_{DP}$

For this threshold value, there is at least one standard deviation of separability for  $SNR \geq 8.0$  dB.

*4.3.5 Dependence of  $\sigma_{AF}$  on SNR, ( $\gamma_{max} < t_\gamma$ ).* The fifth and final key feature considered is  $\sigma_{AF}$ , which is calculated for the two modulations not containing absolute amplitude information (FSK2 and FSK4). Since FSK2 has no absolute frequency information, it can be separated from FSK4, which contains absolute frequency information. Results for 400 realizations are presented in Figure 16, with Figure 17 providing an expanded view. As shown in Figure 17 by the solid horizontal line, a DMRA threshold value for  $\sigma_{AF}$  of  $t_{AF} = 3.3$  is chosen. For this threshold value, there is at least one standard deviation of separability for  $SNR \geq 12.0$  dB. This is clearly the poorest separability of all features considered.

*4.3.6 Summary of Initial DMRA Threshold Values.* The threshold value for each key feature was chosen based on two criteria. First, the threshold is set such

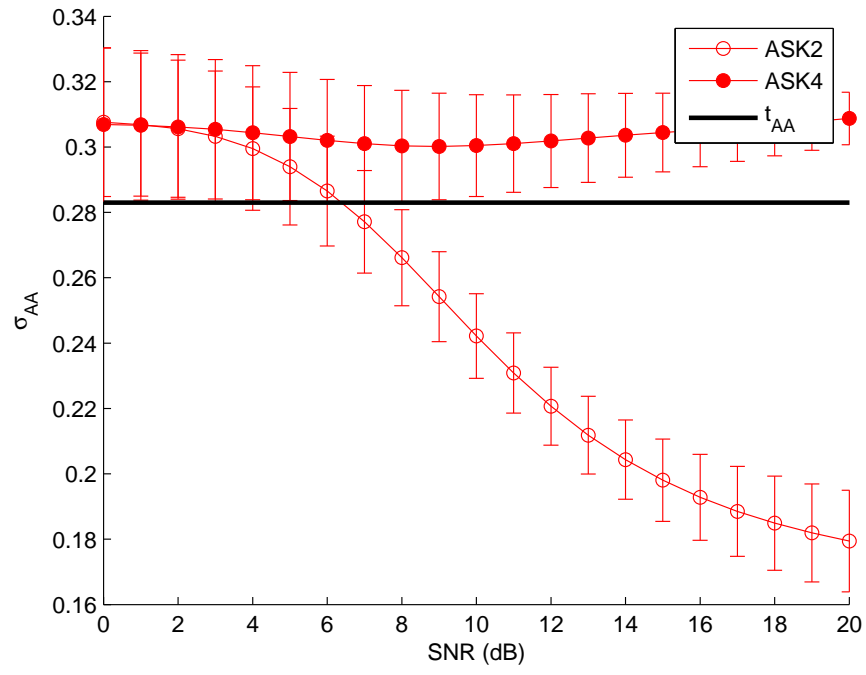


Figure 15: Absolute Amplitude Feature,  $\sigma_{AA}$

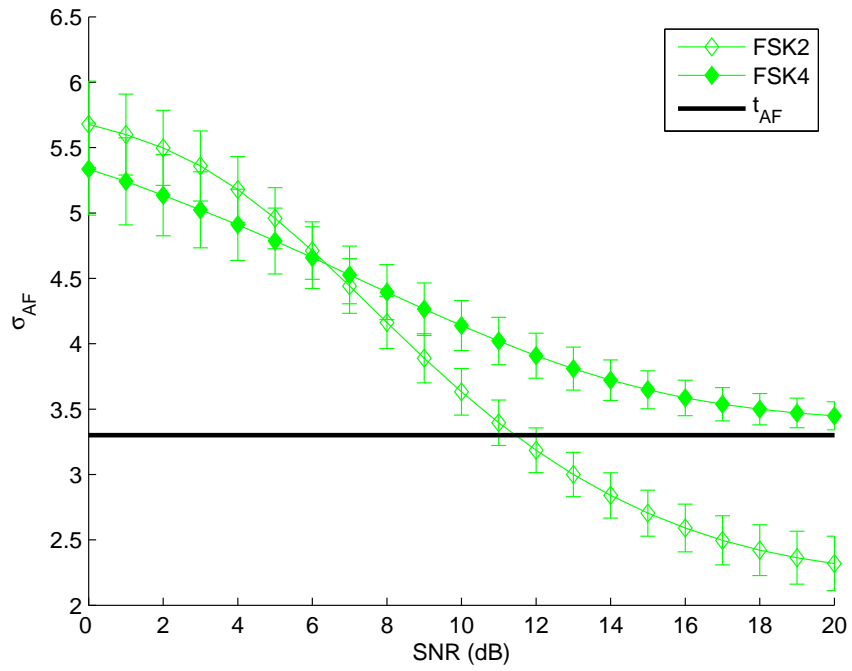


Figure 16: Absolute Frequency Feature,  $\sigma_{AF}$

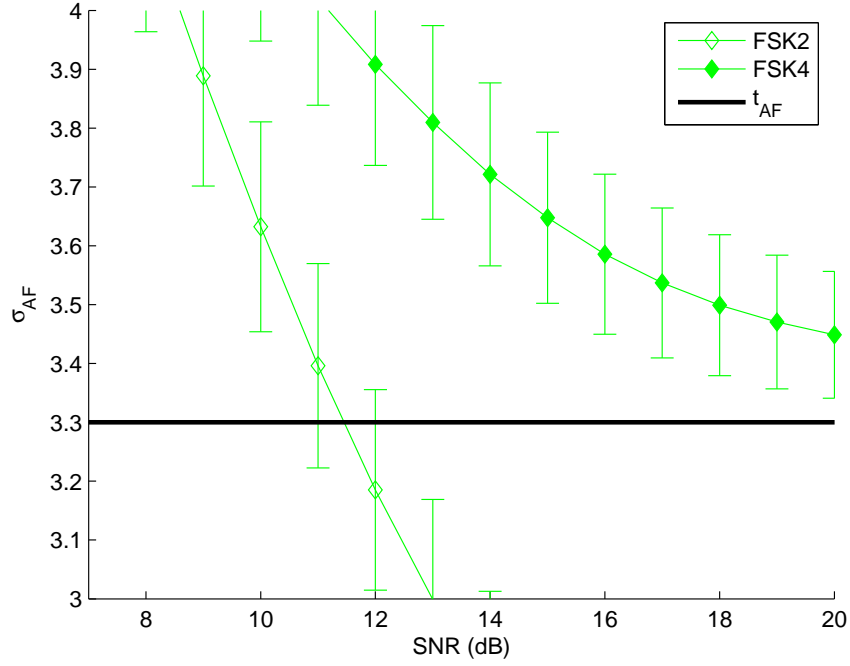


Figure 17: Expanded Plot: Absolute Frequency Feature,  $\sigma_{AF}$

Table 5: Key Feature Threshold Values for Initial DMRA

Key Feature Thresholds	Optimum Value	SNR Limit
$t_\gamma$	2.32	$SNR > 11 \text{ dB}$
$t_{AP}$	0.77	$SNR \geq 0 \text{ dB}$
$t_{DP}$	1.2	$SNR \geq 0 \text{ dB}$
$t_{AA}$	0.283	$SNR \geq 8 \text{ dB}$
$t_{AF}$	3.3	$SNR \geq 12 \text{ dB}$

that the error bars at the lowest SNR value (SNR Limit) do not overlap. Second, the chosen threshold value falls just below the one standard deviation error bar for all SNR values higher than the SNR limit. For example, the SNR limit for  $\gamma_{max}$ , shown in Figure 11, is 11.0 dB. The first criteria is met for a SNR limit of 10 dB; however, moving the threshold up to the 10 dB point would cause the threshold to be within the PSK2 and PSK4 error bars for all SNR values greater than 10.0 dB. Table 5 shows the chosen threshold value and SNR limit for each of the five key features.

Table 6: Fundamental Modulation Confusion Matrix for  $SNR = 10\text{ dB}$  and  $BW = 6 \times r_s$

Simulated Modulation Type	Deduced Modulation Type					
	ASK2	ASK4	PSK2	PSK4	FSK2	FSK4
ASK2	400	0	0	0	0	0
ASK4	27	373	0	0	0	0
PSK2	0	0	399	0	1	0
PSK4	0	0	1	395	4	0
FSK2	0	0	0	300	99	1
FSK4	0	0	0	273	4	123

Table 7: Azzouz and Nandi's Confusion Matrix for  $SNR = 10.0\text{ dB}$  [7]

Simulated Modulation Type	Deduced Modulation Type					
	ASK2	ASK4	PSK2	PSK4	FSK2	FSK4
ASK2	393	7	0	0	0	0
ASK4	0	400	0	0	0	0
PSK2	0	0	397	0	3	0
PSK4	0	0	0	395	5	0
FSK2	0	0	0	2	398	0
FSK4	0	0	0	5	2	393

#### 4.4 Operational DMRA Performance: Fundamental Modulations

The operational DMRA performance is characterized using the chosen feature thresholds and the fundamental modulations under consideration. Confusion matrix results are generated using a given input bandwidth (dictated by the RF filter implementation) and desired SNR value (at the RF filter output).

*4.4.1 Confusion Matrix Analysis.* Table 6 shows confusion matrix results for  $SNR = 10.0\text{ dB}$  using an RF bandwidth equaling six times the symbol rate ( $BW = 6 \times r_s$ ). To compare results shown in Table 6 with results given by Azzouz and Nandi [7], results in Table 3.4 of [7] are converted from percentages to actual occurrences and presented here in Table 7.

In comparing Table 6 and 7 results, it can be seen that the results are consistent with one exception. Results of this work show some confusion exists in calling FSK2

Table 8: Fundamental Modulation Confusion Matrix for  $SNR = 11.0 \text{ dB}$  and  $BW = 6 \times r_s$

Simulated Modulation Type	Deduced Modulation Type					
	ASK2	ASK4	PSK2	PSK4	FSK2	FSK4
ASK2	400	0	0	0	0	0
ASK4	30	370	0	0	0	0
PSK2	0	0	389	0	11	0
PSK4	0	0	42	339	19	0
FSK2	0	0	0	115	285	0
FSK4	0	0	0	160	10	230

and FSK4 as PSK4. In analyzing the cause for this deviation, it was determined that the  $\gamma_{max}$  calculation is most susceptible to noise at lower SNR values, as shown in Figure 11. Setting this deviation aside, the results are consistent both in the confusion matrices and in the feature plots of Figure 10 through Figure 17.

Now that it has been shown that the results for  $SNR = 10.0 \text{ dB}$  are consistent with Azzouz and Nandi [7] (apart from the noted deviation), the DMRA performance is shown to improve (less confusion) at a higher SNR values. For demonstration, an  $SNR = 11.0 \text{ dB}$  is chosen because it includes SNR Limit for  $\gamma_{max}$ , which is the first key feature calculated and primary contributor to the confusion seen in the  $10.0 \text{ dB}$  case. Table 8 shows the confusion matrix for  $SNR = 11.0 \text{ dB}$  and  $BW = 6 \times r_s$ .

#### 4.5 Introduction of QAM-OFDM Waveform

The QAM-OFDM waveform is generated by taking the IFFT of Equation 19. Figure 18 shows the time domain representation of the OFDM waveform over one observation interval,  $T_{obs}$ , containing 20 QAM-OFDM symbols. Figure 19 shows the corresponding amplitude  $a_{cn}$ , phase  $\phi_{NL}$  and  $\phi_{NL2}$  and frequency  $f_N$  functions required for DMRA processing. Most notable in this case is that both the  $a_{cn}$  and  $\phi_{NL}$  functions appear to possess some measurable structure.

*4.5.1 Unmodified DMRA Performance: OFDM Waveform Present.* Operational DMRA performance is first determined with an OFDM waveform input without

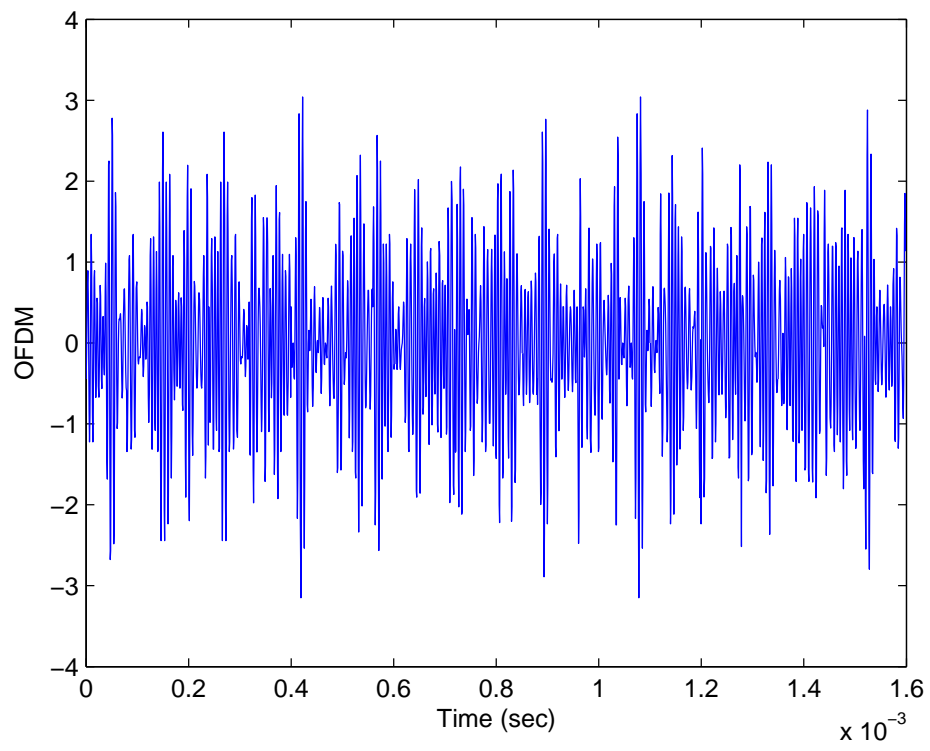


Figure 18: Time Domain OFDM Waveform

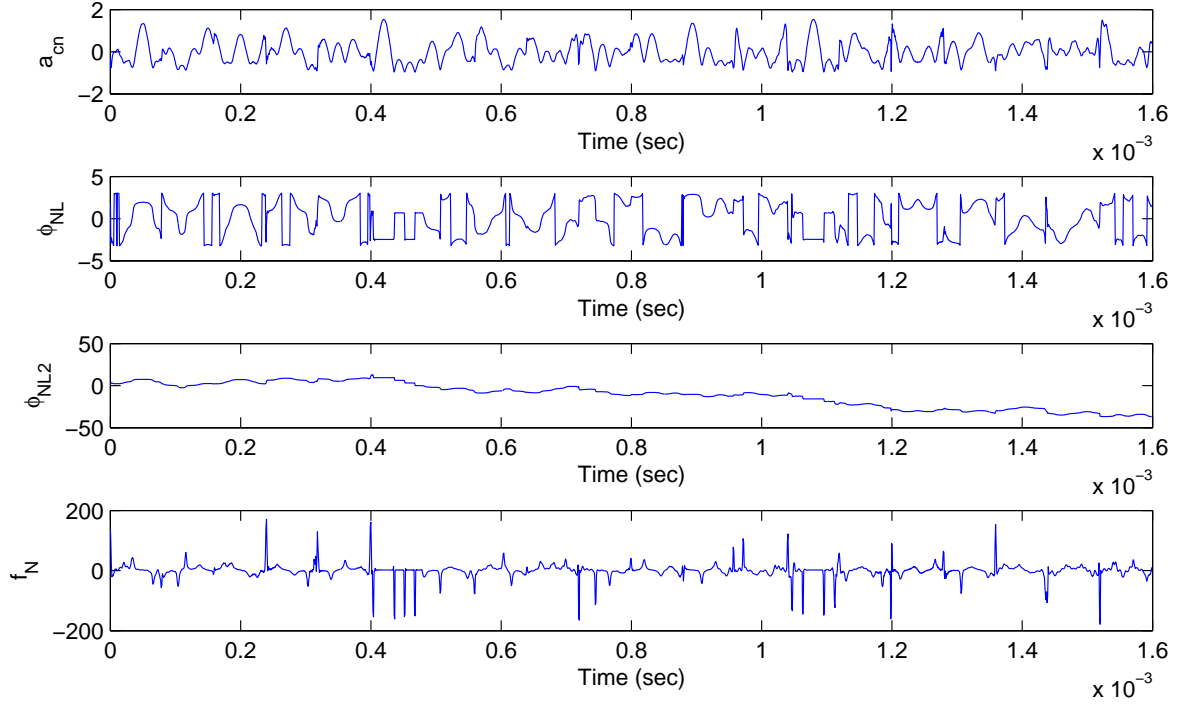


Figure 19: DMRA Features for OFDM Waveform of Figure 18

making any changes to the original DMRA architecture, threshold values of Table 5, or RF bandwidth. The resultant DMRA confusion matrix for this case is shown in Table 9.

*4.5.2 Analysis of Unmodified DMRA with OFDM Waveform.* Table 9 shows that OFDM signal characteristics cause the DMRA to call it PSK4 with nearly 100% certainty (only three instances of it being classified as PSK2). For the DMRA to distinguish OFDM as its own modulation type, another feature or threshold must be created. To determine which DMRA modification is most appropriate, the current feature thresholds were evaluated with the OFDM signal present. Since OFDM is most confused with PSK2 and PSK4, the first threshold evaluated was  $\sigma_{AP}$ . These results are shown in Figures 20, with Figure 21 providing an expanded plot. Figure 21 shows that a new threshold, between PSK4 and OFDM, could be implemented for  $SNR \geq 11.0$  dB.

Table 9: Confusion Matrix for Unmodified DMRA with OFDM Input for  $SNR = 11.0 \text{ dB}$  and  $BW = 6 \times r_s$

Simulated Modulation Type	Deduced Modulation Type					
	ASK2	ASK4	PSK2	PSK4	FSK2	FSK4
ASK2	400	0	0	0	0	0
ASK4	30	370	0	0	0	0
PSK2	0	0	389	0	11	0
PSK4	0	0	42	339	19	0
FSK2	0	0	0	115	285	0
FSK4	0	0	0	160	10	230
OFDM	0	0	3	397	0	0

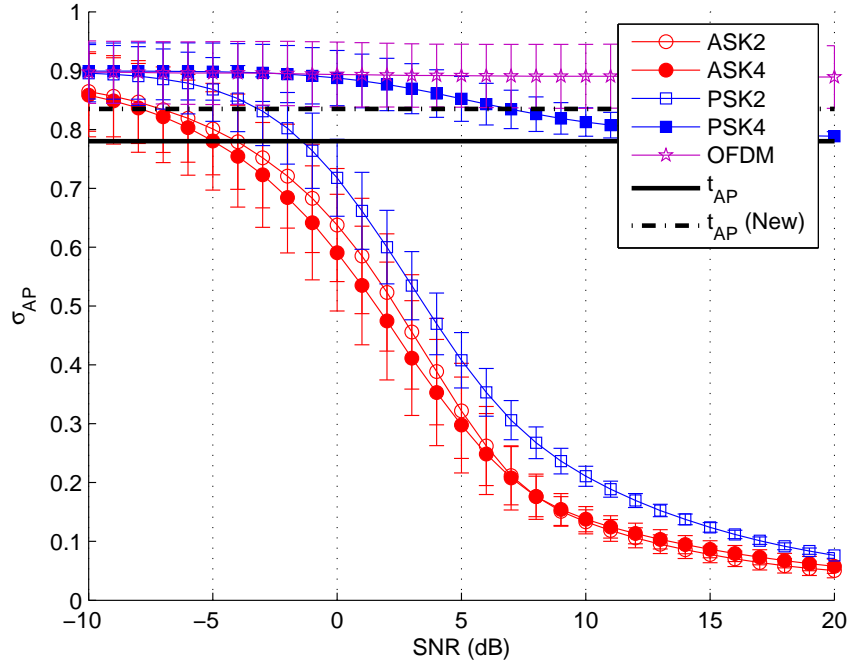


Figure 20: DMRA Absolute Phase Feature,  $\sigma_{AP}$ , with OFDM Waveform Present

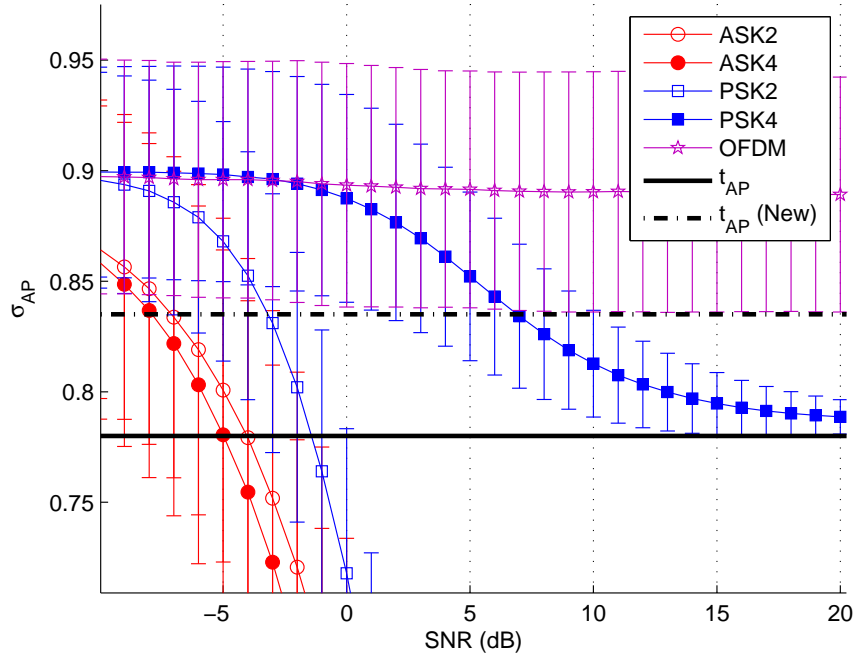


Figure 21: Expanded Plot: DMRA Absolute Phase Feature,  $\sigma_{AP}$ , with OFDM Waveform Present

An alternate implementation involves retaining the original threshold for  $\sigma_{AP}$  and adding an additional key feature. One such option involves adding an additional  $\sigma_{AF}$  feature after the calculation of  $\sigma_{AP}$ . The results for  $\sigma_{AF}$  containing PSK4 and OFDM are shown in Figure 22. The figure shows that a threshold could be chosen such that reliable separability is maintained for  $SNR \geq 5.0 \text{ dB}$ . Given that the SNR limit for adding a new feature is lower than that of adding an addition threshold in  $\sigma_{AP}$ , the new feature  $\sigma_{AF}$  with threshold  $t_{AF(OFDM)}$  is implemented.

*4.5.3 Modified DMRA Performance: OFDM Waveform Present.* The modified DMRA decision tree including OFDM recognition is shown in Figure 23. An updated table of threshold values and SNR limits is provided in Table 10. With the exception of  $t_{AF(OFDM)}$  being added, there are no changes relative to Table 5.

*4.5.4 OFDM Recognition Results.* Table 11 shows confusion matrix results for the modified DMRA with an OFDM signal present. The success rate for classifying

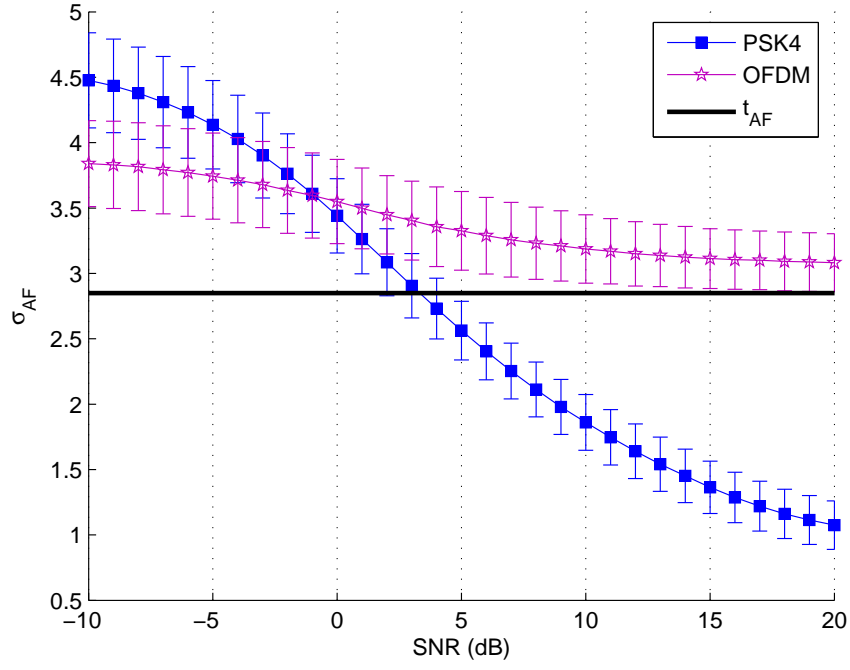


Figure 22: DMRA Absolute Frequency Feature,  $\sigma_{AF}$ , with OFDM Waveform Present

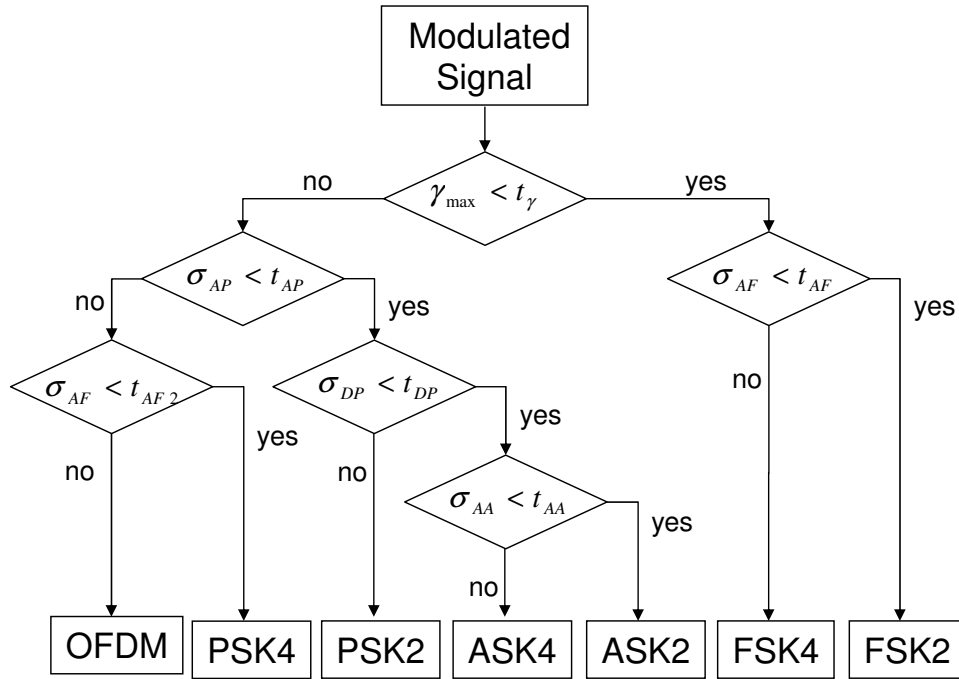


Figure 23: Decision Tree for the Modified DMRA

Table 10: Key Feature Threshold Values for the Modified DMRA

Key Feature Thresholds	Modified Value	SNR Limit
$t_\gamma$	2.32	$SNR > 11 \text{ dB}$
$t_{AP}$	0.77	$SNR \geq 0 \text{ dB}$
$t_{DP}$	1.2	$SNR \geq 0 \text{ dB}$
$t_{AA}$	0.283	$SNR \geq 8 \text{ dB}$
$t_{AF}$	3.3	$SNR \geq 12 \text{ dB}$
$t_{AF(OFDM)}$	2.85	$SNR \geq 5 \text{ dB}$

OFDM signals at 11.0 dB is 95.25%. It should also be noted that the confusion shown in the original DMRA between FSK and PSK has decreased, with FSK now being somewhat confused with OFDM. This result can be attributed to the fact that the FSK signals have higher values in the  $\sigma_{AF}$  feature and are classified with OFDM above the  $t_{AF(OFDM)}$  threshold.

To see how the modified DMRA might perform at lower SNR values, it is next assumed that the input signal is correctly classified (separated) using the  $\gamma_{max}$  feature. This assumption is made to by-pass what appears to be the most significant contributor of confusion given that  $t_\gamma$  separability is limited to  $SNR \geq 11.0 \text{ dB}$ . Under this assumption, the modified DMRA decision tree can be simplified as shown in Figure 24, where only ASK, PSK, and OFDM are recognition options.

Using this limited decision tree, confusion matrix results were generated for  $SNR = 5.0 \text{ dB}$  and  $BW = 6 \times r_s$  and are provided in Table 12. Although confusion remains between ASK2 and ASK4, it can be seen that the performance of the PSK and OFDM signals have improved; the success rate for OFDM is now at 98.25% and the success rates for PSK2 and PSK4 are 100% and 98.25%, respectively.

#### 4.6 Summary

This chapter provides both the developmental and operational performance of the original, modulated, and limited DMRA architectures. The time domain waveforms and detection results are shown for the modulation types considered, including ASK, PSK, FSK, and OFDM. Key features and their associated thresholds are

Table 11: Confusion Matrix with OFDM for  $SNR = 11 \text{ dB}$  and  $BW = 6 \times r_s$

Simulated Modulation Type	Deduced Modulation Type						
	ASK2	ASK4	PSK2	PSK4	FSK2	FSK4	OFDM
ASK2	400	0	0	0	0	0	0
ASK4	58	342	0	0	0	0	0
PSK2	0	0	374	0	26	0	0
PSK4	0	0	3	380	17	0	0
FSK2	0	0	0	13	284	2	101
FSK4	0	0	0	0	24	222	154
OFDM	0	0	2	17	0	0	381

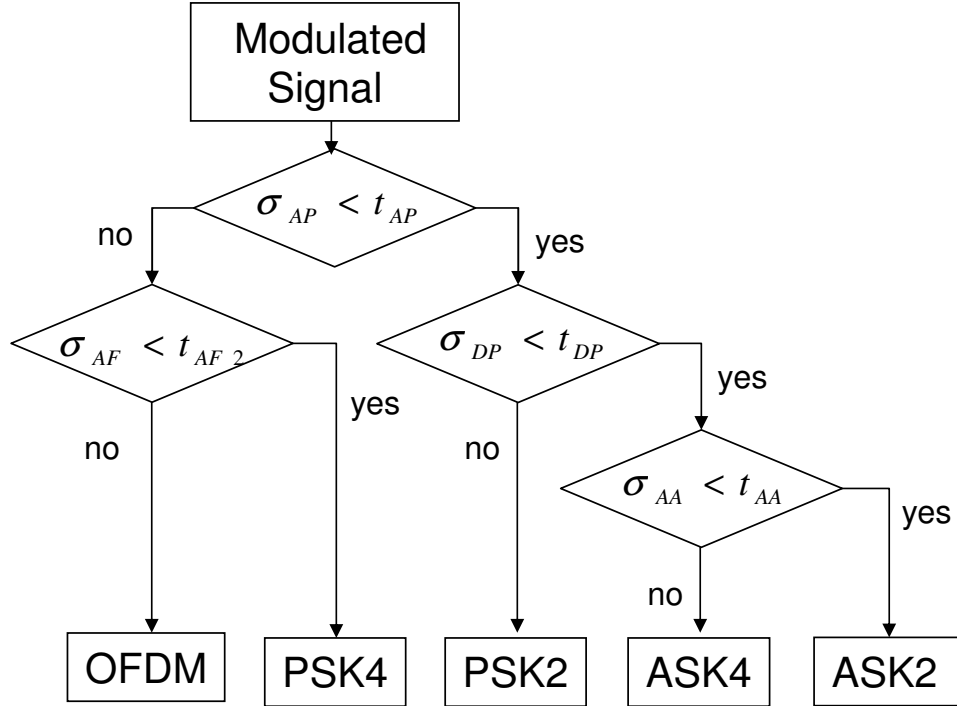


Figure 24: Decision Tree for the Modified DMRA (Limited to ASK, PSK, and OFDM)

Table 12: Limited Confusion Matrix with OFDM for  $SNR = 5.0 \text{ dB}$  and  $BW = 6 \times r_s$

Simulated Modulation Type	Deduced Modulation Type						
	ASK2	ASK4	PSK2	PSK4	FSK2	FSK4	OFDM
ASK2	79	321	0	0	$x$	$x$	0
ASK4	68	332	0	0	$x$	$x$	0
PSK2	0	0	400	0	$x$	$x$	0
PSK4	0	0	0	393	$x$	$x$	7
FSK2	$x$	$x$	$x$	$x$	$x$	$x$	$x$
FSK4	$x$	$x$	$x$	$x$	$x$	$x$	$x$
OFDM	0	0	7	0	$x$	$x$	393

presented along with DMRA performance for specific SNR values. Performance results are represented and analyzed using confusion matrices. It was shown that for the original DMRA architecture, OFDM signals were classified as PSK4 and PSK2. The original DMRA architecture was then modified to incorporate an additional  $\sigma_{AF}$  key feature decision using a new threshold,  $t_{AF(OFDM)}$ , to permit OFDM waveform classification. The modification resulted in a success rate of 95.25% for OFDM classification at an  $SNR = 11.0 \text{ dB}$ . The modified DMRA architecture was then limited by removing the  $\gamma_{max}$  feature (classification of FSK modulation removed) to more fully characterize DMRA OFDM performance at decreased SNR values; this removal increased the OFDM classification success rate to 98.25% at a  $SNR = 5.0 \text{ dB}$ .

## V. Conclusions

### 5.1 Summary

The majority of this research was devoted to developing and characterizing the conventional Digitally Modulated Signal Recognition Algorithm (DMRA) designed by Azzouz and Nandi [7]. The DMRA was originally designed to classify ASK2, ASK4, PSK2, PSK4, FSK2, and FSK4 signals. The original DMRA architecture implemented here yielded performance that was consistent with previously published results.

An Orthogonal Frequency Division Multiplexed (OFDM) waveform was introduced into the original DMRA architecture and its performance was assessed. It was found that the OFDM waveform was most “confused” with the PSK modulations, specifically PSK4. The DMRA architecture was then modified to include a key feature decision and new threshold for OFDM recognition. Using the modified DMRA architecture, it was determined that the OFDM waveform could be successfully classified up to 95.25% of the time for an SNR value of 11.0 dB.

To determine OFDM classification performance at the newly established  $\sigma_{AF(OFDM)}$  limit, the FSK decision option was removed from the DMRA. This operation was simulated by removing the  $\gamma_{max}$  decision and  $\sigma_{AF}$  key features from the right side of the modified DMRA. Limiting the system in this manner improved the overall success rate at an SNR value down to 5.0 dB; success rates of 100% (PSK2), 98.25% (PSK4), and 98.25% (OFDM) were realized.

### 5.2 Recommendations for Future Research

*5.2.1 Improvement of Fundamental Modulation Performance.* In some cases the current DMRA model was found to be quite “sensitive” to input waveform structure. Thus, it would be beneficial to consider the development of a more robust algorithm that is less sensitive for a given waveform type. For example, the current DMRA is “sensitive” to the specific implementation of ASK, i.e., the  $\sigma_{AA}$  calcula-

tion greatly varies based on the coefficients used in Table 2. In most instances, a discernable threshold cannot be found in the  $\sigma_{AA}$  plot.

Changing the order of key features could also be investigated as a means for improving performance. Adjusting the features with higher SNR limits may improve the overall system performance. The order of the features could also be removed from consideration using an artificial neural network. In addition to changing the order of each key feature, new key features could be introduced in the system, which could include moment analysis, power-law classification, zero-crossings, etc.

*5.2.2 Additional Waveform Recognition.* This work only considered ASK2, ASK4, PSK2, PSK4, FSK2, FSK4, and 4-ary QAM-OFDM signals. The DMRA could be expanded to include classification for larger fundamental signal sets. These sets could include M-ary ASK, PSK, and FSK where the value of M is larger than four. The system could also be expanded to include various OFDM signals, such as those used in IEEE 802.11 and 802.16 standards [2,3,5] and those proposed for IEEE 802.15 standards. [4].

The system could also be expanded to include other types of signals, such as Frequency Hopping Spread Spectrum(FHSS), Direct Sequence Spread Spectrum(DSSS), Ultra-Wideband(UWB), and other spectrally encoded systems.

## *Appendix A.*

### ***A.1 4-ary Modulation Waveforms and Instantaneous Plots***

Figure 25 shows representative time domain waveforms for one observation interval,  $T_{obs}$ , consisting of 20 symbols. Results shown in this figure, and subsequent results in Figure 26 through Figure 29, were generated using a random binary sequence of data given by: [01300021021311303223].

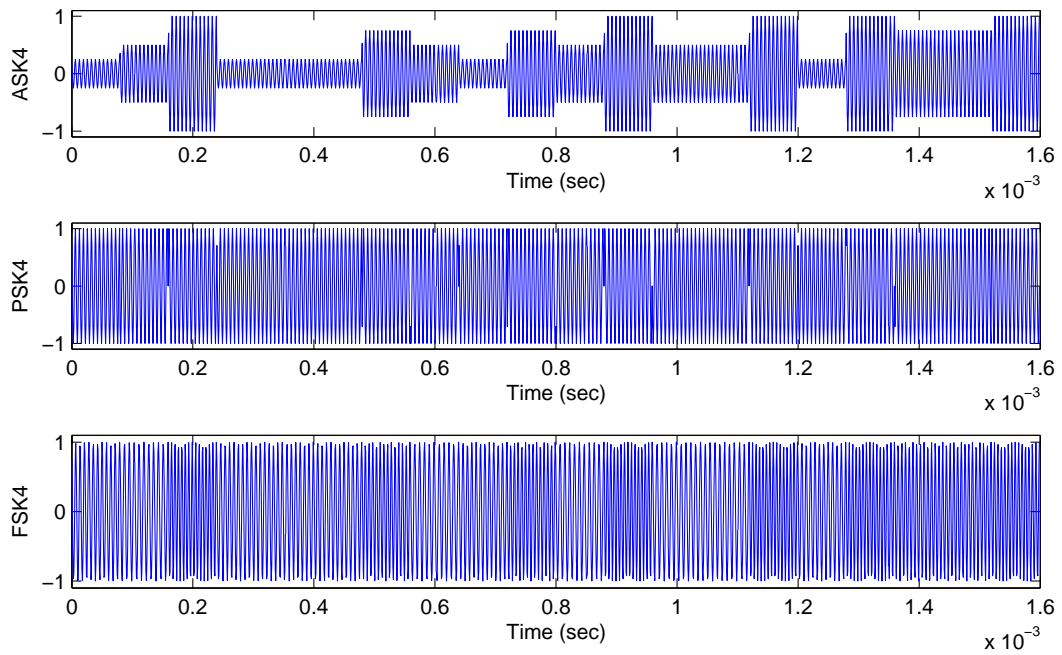


Figure 25: Time Domain Waveforms for 4-ary Modulations

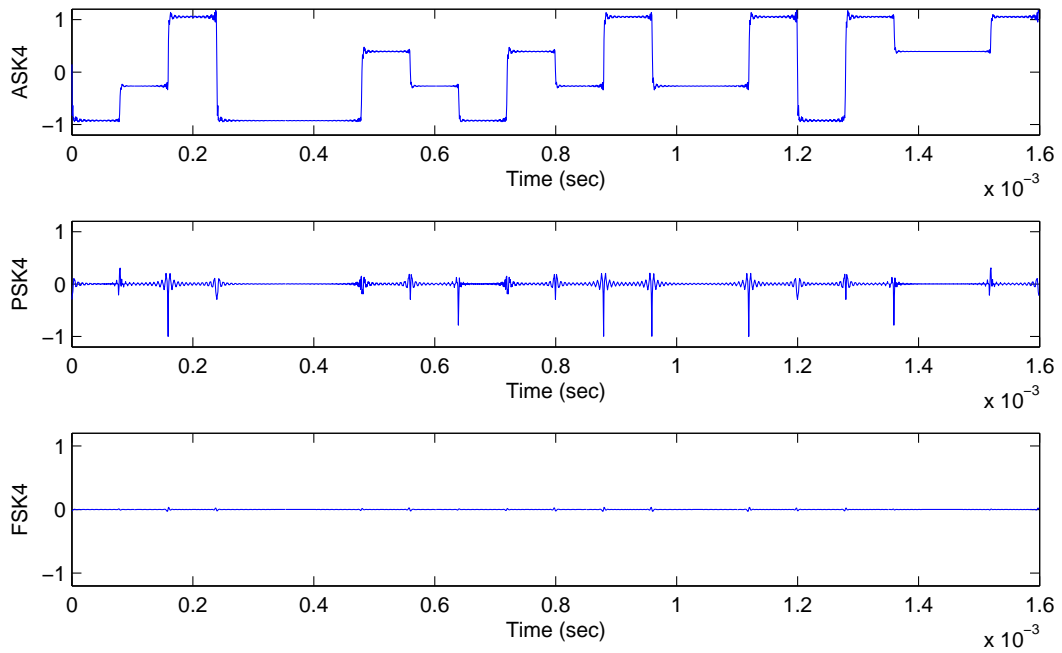


Figure 26: Normalized Centered Instantaneous Amplitude Response,  $a_{cn}$ , for 4-ary Modulated Waveforms of Figure 25

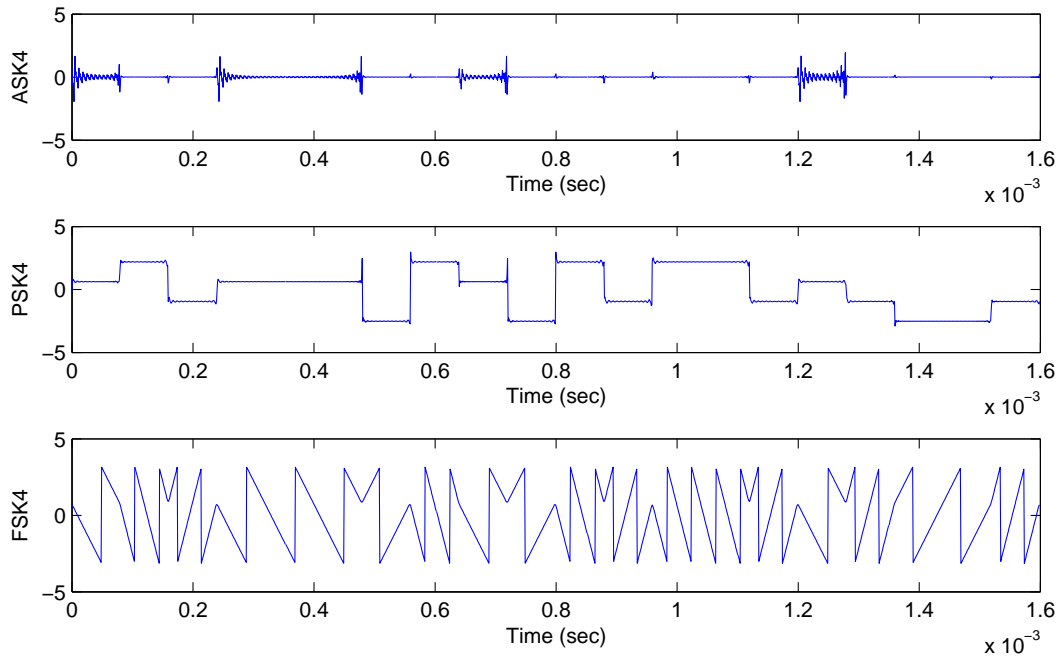


Figure 27: Normalized Centered Nonlinear Phase Response,  $\phi_{NL}$ , for 4-ary Modulated Waveforms of Figure 25

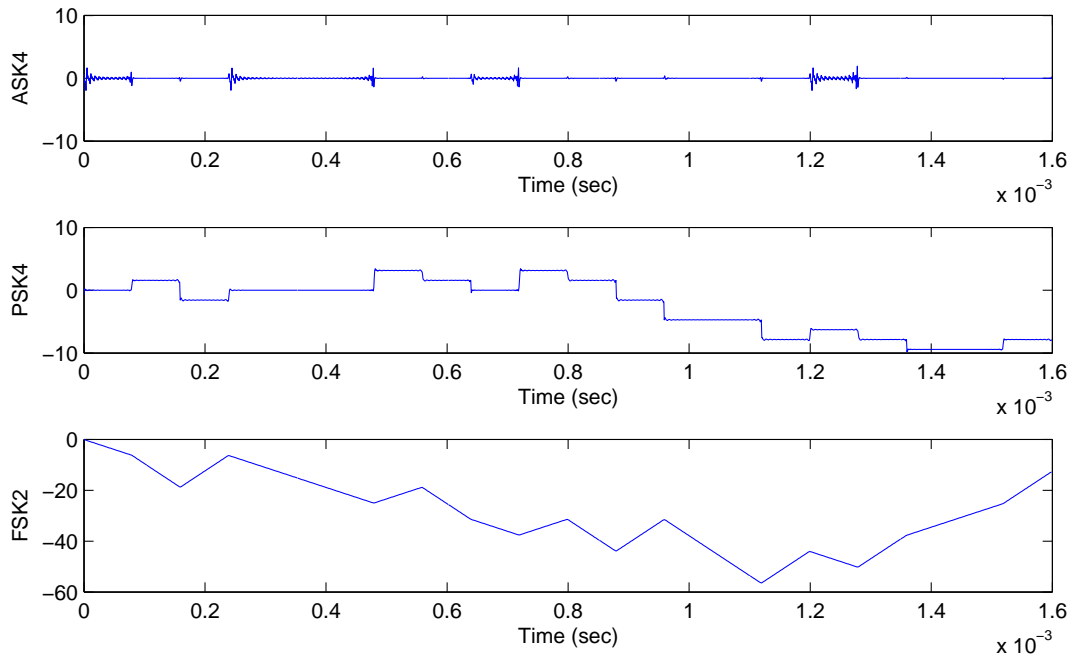


Figure 28: Nonlinear Phase Response,  $\phi_{NL2}$ , for 4-ary Modulated Waveforms of Figure 25

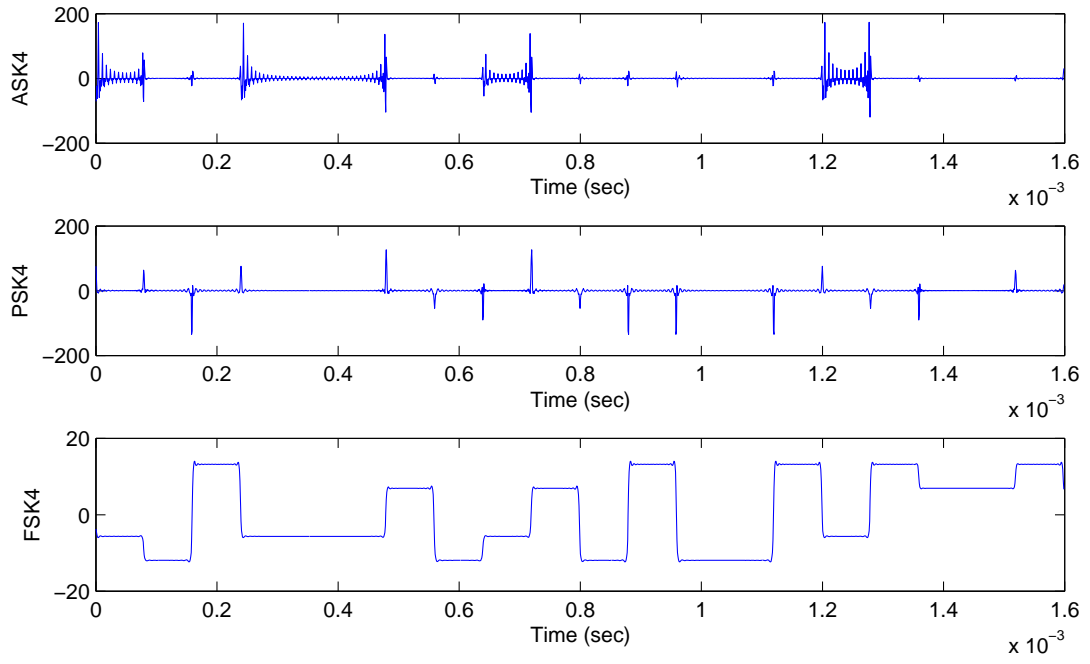


Figure 29: Normalized Centered Frequency Response,  $f_N$ , for Binary Modulated Waveforms of Figure 25

## Bibliography

1. “OFDM for Mobile Data Communications”. International Engineering Consortium Web ProForum Tutorials, <http://www.iec.org/online/tutorials/ofdm>.
2. 802.11a, IEEE. “Wireless LAN Medium Access Control (MAC) and Physical Layer (PHY) Specification: High Speed Physical Layer Extension in the 5 GHz Band”. September 1999.
3. 802.11g, IEEE. “Wireless LAN Medium Access Control (MAC) and Physical Layer (PHY) Specifications, Amendment 4: Further Higher Data Rate Extension in the 2.4 GHz Band”. June 2003.
4. 802.15.3a, IEEE. “IEEE Standard for Information Technology—Telecommunications and Information Exchange Between Systems—Local and Metropolitan Area Networks—Specific Requirements, Part 15.3: Wireless Medium Access Control (MAC) and Physical Layer (PHY) Specifications for High Rate Wireless Personal Area Networks (WPANs)”. September 2003.
5. 802.16a, IEEE. “IEEE Standard for Local and Metropolitan Area Networks— Part 16: Air Interface for Fixed Broadband Wireless Access Systems—Amendment 2: Medium Access Control Modifications and Additional Physical Layer Specifications for 2-11 GHz”. April 2003.
6. Azzouz, E. E. and A. K. Nandi. “Automatic Identification of Digital Modulations”. *Signal Processing*, 47(1):55–69, November 1995.
7. Azzouz, E. E. and A. K. Nandi. *Automatic Modulation Recognition of Communication Signals*. Kluwer Academic Publishers, 1996.
8. Azzouz, E. E. and A. K. Nandi. “Automatic Modulation Recognition - I”. *J. Franklin Institute*, 334B(2):241–273, 1997.
9. Azzouz, E. E. and A. K. Nandi. “Automatic Modulation Recognition - II”. *J. Franklin Institute*, 334B(2):275–305, 1997.
10. Azzouz, E. E. and A. K. Nandi. “Modulation Recognition using Artificial Neural Networks”. *Signal Processing*, 56(2):165–175, 1997.
11. Booth, C. J. *The New IEEE Standard Dictionary of Electrical and Electronics Terms*. The Institute of Electrical and Electronics Engineers, Inc., New York, fifth edition, 1993.
12. Chang, R. W. “Orthogonal Frequency Multiplex Data Transmission System”. Patent 3,488,445, January 1970.
13. DeSimio, M. P. *Automatic Classification of Digitally Modulated Signals*. Master’s thesis, Air Force Institute of Technology, December 1987.

14. DeSimio, M. P. and G. E. Prescott. “Adaptive Generation of Decision Functions for Classification of Digitally Modulated Signals”. *Proceedings of NAECON*, 1010–1014. 1988.
15. Gast, M. S. *802.11 Wireless Networks: The Definitive Guide*. O’Reilly and Associates, Inc., Cambridge, 2002.
16. Liedtke, F. F. “Computer Simulation of an Automatic Classification Procedure for Digitally Modulated Communication Signals with Unknown Parameters”. *Signal Processing*, 6(4):311–323, August 1984.
17. Sklar, B. *Digital Communications: Fundamentals and Applications*. Prentice Hall, New Jersey, 2001.
18. Su, W. and J. Kosinski. “A Survey of Digital Modulation Recognition Methods”. International Signals Processing Conference, Dallas, TX, April 2003.
19. Weaver, C. S., C. A. Cole, R. B. Krumland, and M. L. Miller. *The Automatic Classification of Modulation Types by Pattern Recognition*. Technical Report 1829-2, Air Force Avionics Laboratory, Wright-Patterson AFB, OH, April 1969.

<b>REPORT DOCUMENTATION PAGE</b>					<i>Form Approved</i> <i>OMB No. 0704-0188</i>	
The public reporting burden for this collection of information is estimated to average 1 hour per response, including the time for reviewing instructions, searching existing data sources, gathering and maintaining the data needed, and completing and reviewing the collection of information. Send comments regarding this burden estimate or any other aspect of this collection of information, including suggestions for reducing this burden to Department of Defense, Washington Headquarters Services, Directorate for Information Operations and Reports (0704-0188), 1215 Jefferson Davis Highway, Suite 1204, Arlington, VA 22202-4302. Respondents should be aware that notwithstanding any other provision of law, no person shall be subject to any penalty for failing to comply with a collection of information if it does not display a currently valid OMB control number. <b>PLEASE DO NOT RETURN YOUR FORM TO THE ABOVE ADDRESS.</b>						
<b>1. REPORT DATE</b> (DD-MM-YYYY) 21-03-2005		<b>2. REPORT TYPE</b> Master's Thesis		<b>3. DATES COVERED</b> (From — To) Sept 2003 — Mar 2005		
<b>4. TITLE AND SUBTITLE</b>  Modification of a Modulation Recognition Algorithm to Enable Multi-Carrier Recognition				<b>5a. CONTRACT NUMBER</b>		
				<b>5b. GRANT NUMBER</b>		
				<b>5c. PROGRAM ELEMENT NUMBER</b>		
				<b>5d. PROJECT NUMBER</b>		
<b>6. AUTHOR(S)</b>  Waters, Angela M., 2LT, USAF				<b>5e. TASK NUMBER</b>		
				<b>5f. WORK UNIT NUMBER</b>		
<b>7. PERFORMING ORGANIZATION NAME(S) AND ADDRESS(ES)</b> Air Force Institute of Technology Graduate School of Engineering and Management 2950 Hobson Way, Bldg 641 WPAFB OH 45433-7765				<b>8. PERFORMING ORGANIZATION REPORT NUMBER</b>  AFIT/GE/ENG/05-23		
<b>9. SPONSORING / MONITORING AGENCY NAME(S) AND ADDRESS(ES)</b> AFRL/SNRW Attn: Dr. James P. Stephens 2241 Avionics Circle Wright Patterson Air Force Base, OH 45433 (937) 255-5579, ext 3547 James.Stephens@wpafb.mil				<b>10. SPONSOR/MONITOR'S ACRONYM(S)</b>		
				<b>11. SPONSOR/MONITOR'S REPORT NUMBER(S)</b>		
<b>12. DISTRIBUTION / AVAILABILITY STATEMENT</b>  Approval for public release; distribution is unlimited.						
<b>13. SUPPLEMENTARY NOTES</b>						
<b>14. ABSTRACT</b> Modulation recognition is important for both military and commercial communication applications, particularly in cases where enhanced situation awareness and/or channel assessment is required to mitigate intentional or collateral interference. Modulation recognition via statistical analysis is a key aspect of non-cooperative signal interception, classification, and exploitation. This research concerns the evaluation and modification of a conventional Digitally Modulated Signal Recognition Algorithm (DMRA) to enable multi-carrier, OFDM, waveform recognition. The original DMRA architecture was developed to classify communication signals for three fundamental data modulations, i.e., ASK, PSK, and FSK. By adding an additional key feature and threshold to the original DMRA architecture, a modified DMRA architecture is developed to enable the reliable recognition of OFDM waveforms. Simulation results for the modified DMRA architecture show a 95.25% success rate for OFDM waveform recognition at a signal-to-noise ratio (SNR) of 11.0 dB. When operated under scenarios where FSK signals are neither present nor considered an alternative, the modified DMRA architecture yields a success rate of 98.25% for classifying OFDM at a SNR of 5.0 dB.						
<b>15. SUBJECT TERMS</b>  Pattern Recognition, Feature Extraction, Amplitude Modulation, Phase Modulation, Frequency Modulation, Communication Networks						
<b>16. SECURITY CLASSIFICATION OF:</b>			<b>17. LIMITATION OF ABSTRACT</b>	<b>18. NUMBER OF PAGES</b>	<b>19a. NAME OF RESPONSIBLE PERSON</b>	
a. REPORT	b. ABSTRACT	c. THIS PAGE			Dr. Michael A. Temple, AFIT/ENG	
U	U	U	UU	63	<b>19b. TELEPHONE NUMBER</b> (include area code) (937) 255-6565x4279, Michael.Temple@afit.edu	